IRREGULAR REPETITION SLOTTED ALOHA WITH ENERGY HARVESTING NODES

A THESIS SUBMITTED TO

THE GRADUATE SCHOOL OF ENGINEERING AND SCIENCE

OF BILKENT UNIVERSITY

IN PARTIAL FULFILLMENT OF THE REQUIREMENTS FOR

THE DEGREE OF

MASTER OF SCIENCE

IN

ELECTRICAL AND ELECTRONICS ENGINEERING

By

Umut Demirhan

July 2017

Irregular Repetition Slotted ALOHA with Energy Harvesting Nodes

By Umut Demirhan

July 2017

We certify that we have read this thesis and that in our opinion it is fully adequate, in scope and in quality, as a thesis for the degree of Master of Science.

Tolga Mete Duman (Advisor)

Ezhan Karaşan

Mehmet Köseoğlu

Approved for the Graduate School of Engineering and Science:

Ezhan Karaşan
Director of the Graduate School

ABSTRACT

IRREGULAR REPETITION SLOTTED ALOHA WITH ENERGY HARVESTING NODES

Umut Demirhan
M.S. in Electrical and Electronics Engineering
Advisor: Tolga Mete Duman
July 2017

The importance of wireless networking schemes originating from ALOHA has rapidly risen with the wide-spread use of Internet, advancements in the communications systems and increasing number of wireless devices. Internet-of-Things and machine-to-machine communications concepts have drawn further attention to ALOHA since it is a low-complexity protocol. However, the classical ALOHA is not efficient and cannot handle massive number of users in an efficient manner. Therefore, many improvements have been proposed for over the years.

Irregular Repetition Slotted ALOHA (IRSA) is an advanced ALOHA protocol in which each user sends a variable number of copies of their packets in each fixed length medium access control (MAC) frame. The collisions may be resolved via successive interference cancellation (SIC) using the copies that are received cleanly. In this way, asymptotic throughputs close to the maximum normalized throughput value of one on the collision channel may be achieved.

In this thesis, to reap the benefits of IRSA for energy harvesting sensor networks, we propose an IRSA based uncoordinated random access scheme for energy harvesting (EH) nodes. Specifically, we consider the case in which each user has a finite-sized battery which is recharged in a probabilistic manner in each slot with harvested energy from the environment. We analyze this scheme by deriving asymptotic throughput expressions, and obtain optimized probability distributions for the number of packet replicas for each user. We demonstrate that the optimized distributions perform considerably better than those of slotted ALOHA (SA), contention resolution diversity slotted ALOHA (CRDSA) and plain IRSA which do not take into account EH for both asymptotic and finite frame length scenarios.

Keywords: ALOHA, M2M communications, energy harvesting, random access, sensor networks, throughput optimization.

ÖZET

ENERJİ HASATLAYAN DÜĞÜMLERLE DÜZENSİZ TEKRARLI DİLİMLİ ALOHA

Umut Demirhan
Elektrik ve Elektronik Mühendisliği, Yüksek Lisans
Tez Danışmanı: Tolga Mete Duman
Temmuz 2017

ALOHA'dan beri süregelen kablosuz ağ protokollerinin önemi, internetin yaygın şekilde kullanımı, iletişim sistemlerindeki gelişmeler ve artan sayıda kablosuz iletişim cihazları gibi sebeplerden dolayı hızlı bir şekilde artmıştır. Nesnelerin interneti (IoT) ve makineler arası (M2M) iletişim kavramları düşük karmaşıklıklı bir protokol olan ALOHA'ya olan ilgiyi arttırmıştır. Buna karşın klasik ALOHA verimli bir protokol değildir ve çok sayıda kullanıcıyı da etkin şekilde destekleyemez. Bu nedenle, yıllar içinde ALOHA'nın verimlileştirilmesi için birçok çalışma yapılmıştır.

Düzensiz Tekrarlı Dilimli ALOHA (IRSA), her kullanıcının sabit uzunluktaki orta erişim denetimi (MAC) çerçevelerinde göndermek istedikleri paketlerinin çeşitli sayıdaki kopyalarını gönderdiği gelişmiş bir ALOHA protokolüdür. Çarpışmalar, alıcıdaki çarpışma olmadan alınan kopyaları kullanarak ardışık girişim iptali (SIC) ile çözülebilir. Bu şekilde, çarpışma kanalında maksimum normalize edilmiş verimlilik olan bir değerine asimptotik olarak yakın değerler elde edilebilir.

IRSA'nın avantajlarını enerji hasatlayan algılayıcı ağlara uygulayabilmek adına enerji hasatlayan düğümler için bir IRSA temelli koordine edilmemiş rastgele erişim şeması öneriyoruz. Özellikle, her kullanıcının çevresinden hasat ettiği enerji ile her dilimde olasılıksal olarak doldurduğu belirli boyutlu bir pile sahip olduğu bir sistemi ele alıyoruz. Bu şemayı asimptotik verimlilik ifadelerini türeterek analiz ediyoruz ve paket kopya sayısı için optimize edilmiş olasılık dağılımları üretiyoruz. Son olarak bu dağılımların, enerji hasatlamayı dikkate almayan dilimli ALOHA, iki paket kopyası gönderilen tekrarlı şema ve normal IRSA dağılımlarından asimptotik ve sonlu çerçevelerde daha iyi çalıştığını gösteriyoruz.

Anahtar sözcükler: ALOHA, makineler arası iletişim, enerji hasatlama, rastgele erişim, algılayıcı ağlar, verimlilik iyileştirmesi.

Acknowledgement

First and foremost, I would like to express my deepest gratitude to my supervisor Prof. Tolga Mete Duman for his continuous support, patience and encouragement for the research and my self improvement. His invaluable experience and guidance have been of great importance to me.

I would also like to thank Prof. Ezhan Karaşan and Assist. Prof. Mehmet Köseoğlu as my examining committee members and for providing constructive comments.

I would like to extend my deepest gratitude to my beloved family who have always supported me in every possible way.

I would like to thank my close friends Nurullah Karakoç, Kaan and Hakan Gökcesu for their fruitful discussions and help in the progress of my research.

I would also like to express my thanks to my office mates Sina Rezaei Aghdam, Mehdi Dabirnia, Alireza Nooraiepour, Serdar Hanoğlu, Mahdi Shakiba Herfeh and Ersin Yar for sharing their knowledge and providing their assistance.

I would like to acknowledge the financial support of the Scientific and Technological Research Council of Turkey (TÜBİTAK) during my M.Sc. studies in parts under the grant 113E223 and BİDEB 2210-A Scholarship Programme with sincere gratitudes.

Contents

List of Figures

List of Tables

List of Abbreviations

BN Burst Node.

CRDSA Contention Resolution Diversity Slotted ALOHA.

CSA Coded Slotted ALOHA.

DFSA Dynamic Frame Slotted ALOHA.

EH Energy Harvesting.

ERD Effective Repetition Distribution.

IoT Internet-of-Things.

IRSA Irregular Repetition Slotted ALOHA.

LDPC low-density parity-check.

M2M Machine-to-Machine.

MAC Medium Access Control.

MTC Machine-Type Communications.

MTD Machine-Type-Device.

PLR Packet Loss Ratio.

RA Random Access.

RD Repetition Distribution.

RF Radio Frequency.

SIC Successive Interference Cancellation.

SN Sum Node.

SNR Signal to Noise Ratio.

Chapter 1

Introduction

1.1 Overview

The importance of wireless networking schemes originating from ALOHA has rapidly risen with the wide-spread use of Internet, advancements in the communications systems and increasing number of wireless devices. The first of its kind, ALOHA, is developed to connect different campuses and research centers of University of Hawaii to the main computing center in 1970 [1]. In this scheme, more recently referred to as pure ALOHA, the messages sent to the main computing center are considered as bursts and each user is allowed to send its packets as it needs to. This scheme constructs a random communications scheme whose efficiency of channel usage (throughput) is determined by a probabilistic analysis leading many works to develop random access (RA) schemes with improved performance. Slotted ALOHA [2] is such an advancement that doubles the throughput by reducing probability of collisions by half with the use of slot synchronization.

Recently, Internet-of-Things (IoT) [3] which is the concept of connecting variety of objects including sensors, actuators, mobile phones etc. by enabling cooperation among them to achieve common objectives, has drawn strong attention to

ALOHA. Machine-type communications (MTC) or Machine-to-Machine (M2M) communications is an important element of the IoT concept that examines the communications between machine-type-devices (MTDs). With the drastic growth of IoT, we expect massive number of MTDs that require new communication standards and network protocols. That is, for the fifth generation mobile technology (5G) and beyond, MTC schemes providing low latencies, greater throughputs and high reliabilities with much higher densities are needed [4]. Therefore, the significance of RA schemes has risen since such techniques have great potential to provide stable networks with high throughputs and low-complexities. To this end, system sum throughput optimization of RA schemes, consequently the number of users supported by the network is an important research topic to be investigated.

Many studies deal with the stable throughput optimization problem of ALOHA-type communication schemes, by proposing modifications or variations to pure ALOHA improving efficiency of this scheme, e.g., [2, 5–8]. In this direction, Irregular Repetition Slotted ALOHA (IRSA) [8] has shown promising results preserving the random nature of the transmissions and pushing the throughput to the maximum value of 1 successful packet transmission per slot asymptotically over the simple collision channel.

It is also of interest to devise MTC systems that function for a very long time, therefore MTDs should be equipped with energy harvesting (EH) capabilities to operate without the need for battery replacement. Accordingly, the IRSA scheme and its benefits can potentially be adopted for the EH setting where MTDs have the ability to harvest energy from the environment which could be via wind, light, vibration, radio frequency (RF) signals etc. enabling perpetual wireless networks. With this motivation, our main concern in this thesis is to develop an IRSA based scheme accommodating EH nodes and its optimization for improving the system throughput.

1.2 Literature Review

ALOHA is the pioneer networking scheme [1] in which when a user has a packet to send, it sends it immediately after the random packet arrivals, without any control protocol or state information of the other users. The working principle of ALOHA relies on the following: the message packets are short, hence they can be considered as bursts and collision probabilities of these bursts are low. In ALOHA and its variants, throughput is used as the main performance measure which is the number of successful packets sent per unit time. With ALOHA, a maximum throughput of $T = 1/2e \approx 0.18$ is obtained.

After the pure ALOHA, another approach, slotted ALOHA, came up [2]. In this scheme, time is split into time-slots in the fixed length of packets and each user sends its packets in exact time slots only. Although a clock synchronization is required in this system, i.e., the system is somewhat more complex, it is easily implementable via sending and receiving a single message. The maximum throughput of slotted ALOHA is twice of the one with the pure ALOHA, i.e., $T = 1/e \approx 0.37$ packets/slot.

In [6], time and frequency diversity in pure and slotted ALOHA are investigated. Packet repetition is considered to provide diversity. Contention Resolution Diversity Slotted ALOHA (CRDSA) [7] proposes a more efficient use of packet repetition by employing SIC among the slots to resolve the collisions at the receiver. Specifically, some number of slots are grouped as medium access control (MAC) frames, and within each frame, each user sends two copies of its packet in randomly selected time slots. In this scheme, the collision channel is considered where slots with a single replica are always successfully decoded while collisions are considered as non-resolvable, i.e., no information can be obtained from the collision in the absence of any additional knowledge. The collisions are resolved by subtracting a decoded packet from another occurrence of that packet. This procedure is applied iteratively with the aim to resolve all the collisions. The resulting throughput is up to $T \simeq 0.55$ packets/slot.

After representing the SIC process explicitly on a bipartite graph, Liva proposes to vary the number of repetitions according to a probability distribution in [8] resulting in IRSA. The SIC process is similar to the decoding of low-density parity-check (LDPC) codes allowing for the use of the tools from LDPC coding literature for analysis and optimization. Therefore, an iterative process similar to the density evolution of LDPC codes to analyze the asymptotic performance of the scheme for a fixed repetition distribution is derived. In this way, it is possible to optimize the repetition distribution using a differential evolution algorithm [9], resulting in IRSA schemes with a maximum asymptotic throughput of $T \simeq 0.97$ packets/slot and practical throughput of $T \simeq 0.8$ packets/slot.

The authors in [5, 10] introduce Coded Slotted ALOHA (CSA) by extending IRSA to send coded packet segments instead of sending replicas of complete packets which can be considered as a generalization of the repetition code used in [8]. In this scheme, each slot and packet are divided into k segments and each packet is randomly coded with a code of rate $R = \frac{k}{n}$ where n is drawn from a probability distribution for each user in each frame. The convergence analysis of IRSA is extended for this scheme. With an optimization algorithm via density evolution, it is shown that the CSA provides a maximum asymptotic throughput of 1 packets/slot with average code rate limitations.

Although the asymptotic throughput optimization on the collision channel with CSA results in a maximum channel efficiency (throughput) of 1 packets/slot, it is not an accurate model for detailed physical layer channel studies. With this motivation, in [11, 12], error analysis and optimization studies over erasure channels are provided. Moreover, with a complex channel model, slots can be considered as multiple-access channels and throughputs greater than 1 packets/slot become achievable. In [13, 14], the authors propose to encode the messages and split the encoder outputs into segments, and then try to decode the received messages carrying the segments together (even with interference, differently from CSA). In this way, with the aid of the physical layer and the channel model, a maximum throughput higher than 1 packets/slot is achieved. In this direction, different channel models such as erasure channel, fading channel, and optimization of CSA are considered in some other recent works [15–20].

A general review of the current status of EH wireless communications can be found in [21]. This paper examines the state of art wireless networks with EH nodes starting with an information theoretical perspective. RA schemes with EH nodes are studied extensively as well. The two-user energy limited RA with multi-packet reception capability is investigated for its stability from an information theoretic perspective in [22, 23]. In [24], the stability of slotted ALOHA with opportunistic RF EH is studied. The authors in [25, 26] study the sum throughput of slotted ALOHA and its optimization with varying transmission power levels depending on the EH rate and battery properties. A game theoretic optimal strategy on the decision of waiting to send a packet at a later time or to send it immediately, for random multiple-access with EH nodes is presented in [27]. Dynamic Frame Slotted ALOHA (DFSA) with EH is proposed in [28]. In this work, DFSA [29] in which the length of the frames are adjusted depending on the collided, successful and empty slots, is adopted for an energy-constrained system with EH nodes. The same authors compare the EH performance of DFSA and frame slotted ALOHA with time-division multiple access and show the performance improvement of dynamic frame length in terms of delivery probability and time efficiency in [30]. In [31], the users are grouped according to their energy availability and DFSA with EH is optimized for throughput and delivery error ratio. In [32], DFSA is analyzed for M2M networks by taking battery and minimum energy limits into consideration. Reservation dynamic frame slotted ALOHA considers reserving slots for the users [33]. The slots that users transmit their packets successfully, are allocated for the same users in the next frames preventing the others to send packet in that slot and cause a collision.

1.3 Thesis Contributions

The main contribution of the thesis is the following: we adopt IRSA for EH nodes and derive convergence analysis expressions to optimize the proposed scheme for throughput. Therefore, we propose a modified IRSA scheme accommodating EH nodes named as Energy-Harvesting Irregular Repetition Slotted ALOHA (EH-IRSA). In the proposed scheme, sporadically activated users with EH capabilities are equipped with a battery that can provide energy for a finite number of packet transmissions. Users draw the number of replicas for their packets from a probability distribution and select specific time slots to send them across a frame, similar to IRSA. On the other hand, if a user has no energy in its selected slot, transmission cannot take place, hence the allocated slot is skipped.

In our model, we assume that a unit cell, that provides energy for only one packet transmission, of the battery is recharged with a certain probability in each slot, independently of the other slots and users. We first consider a unit-sized battery for each user, and analyze the asymptotic throughput of the system for a fixed EH rate which is defined as the expected number of energy arrivals in a frame. Then, we extend our formulation for users with larger battery capacities and develop an analytical methodology to obtain the asymptotic performance. For both cases, we show that the finite MAC frame length throughput performances conform with the theoretical (asymptotic) results.

We utilize the derived expressions for both the unit and finite-sized battery scenarios to find the optimal degree distributions for packet replicas via density evolution for different EH rates. While the results of the unit-battery case are obtained by a fully analytic approach, for higher battery capacity, a solution provided by a more complex analytical methodology and Monte Carlo simulations are employed. Our numerical results demonstrate the superiority of the proposed solutions both asymptotically and through extensive finite frame length simulations.

1.4 Thesis Outline

The thesis is organized as follows: in Chapter 2, ALOHA, slotted ALOHA and IRSA with their mathematical models and some simulation results are given as background for the following chapters. In Chapter 3, we propose an adaptation of IRSA for EH nodes to optimize the throughput in an EH based wireless network. We analyze and optimize the throughput performance of the proposed system on the simple collision channel where a binary EH model in which a unit-sized battery is recharged with a fixed probability in each slot is considered. We analytically derive the convergence analysis expressions and optimize the repetition distributions for the EH case. We also present numerical results of the convergence analysis and compare them with finite length simulation results. In Chapter 4, we extend our approach for the unit-sized battery capacity to the case with a finite battery capacity. In this case, we propose an analytical methodology to obtain the asymptotic results for the given EH rate, and optimize the repetition distributions to maximize the system throughput. We finally compare the asymptotic and finite frame length simulations to examine the efficiency of the methodology. In Chapter 5, conclusions are drawn and some promising future research directions are given.

Chapter 2

Preliminaries

In this chapter, we provide the preliminaries required for an understanding of the rest of the thesis. Throughput optimization is an important concept we aim, thus, the simple base lines, pure ALOHA and slotted ALOHA are explained with the relevant mathematical models, and their throughput results are presented. The material in both Chapter 3 and 4 rely on IRSA, hence IRSA is presented in detail as well.

The chapter is organized as follows. In Section 2.1, the pure ALOHA scheme is described. Slotted ALOHA is presented in Section 2.2. In Section 2.3, IRSA is covered with the details of its model, the optimization methodology and the simulation results. The chapter is concluded with a summary in Section 2.4.

2.1 Pure ALOHA

In pure ALOHA, the first of RA schemes, each user sends its packets without a control as it needs to. In other words, packets arrive to users, and users send their packets without waiting. If packets of different users collide at the receiver, those packets are not resolved. Therefore, an acknowledgment is not received by the users and they send their packets again after some random waiting time. Let

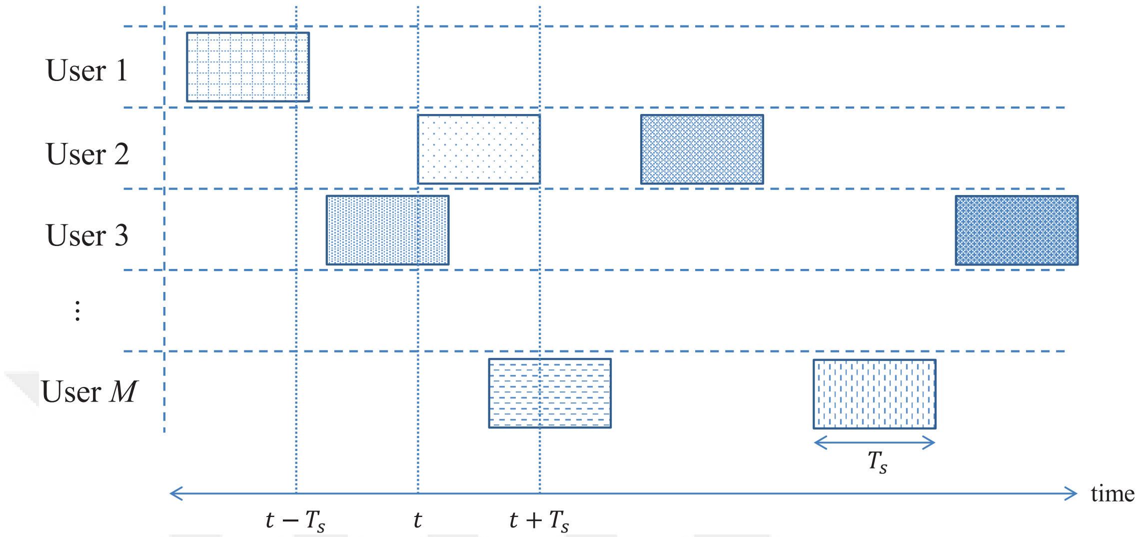

Figure 2.1: The pure ALOHA scheme from a user-time perspective.

us denote the channel load on average in packets sent per unit time by G, and the throughput which is the number of cleanly received packets per unit time by T where unit time is considered as the length of a packet. Each packet length is T_s. We consider a user starting to send a packet at time t. If another user tries to send a packet in the interval $(t - T_s, t + T_s)$, these packets collide, and the users retransmit their packets at another time. An example can be seen in Figure 2.1 where User 3 starts to send a packet in the interval $(t - T_s, t)$ and User M starts to send a packet in the interval $(t, t + T_s)$. Both of these packets collide with the first packet of User 2 which begins at time t.

From the perspective of a given user, when a specific packet is transmitted, there needs to be no transmission in an interval of length $2T_s$ so as to avoid a collision. The arrivals are Poisson random variables, and for the probability of no arrivals except the one we consider, we have $\frac{(2G)^k e^{-2G}}{k!}$ evaluated at $k = 0$ resulting in the probability of no collisions as e^{-2G}. Then we multiply probability of no collision (success) with the density of users, and obtain a throughput of $T = Ge^{-2G}$. By differentiation with respect to G, it can be seen that the throughput is maximized at $G = 0.5$, and the maximum throughput is $1/2e$.

2.2 Slotted ALOHA

In slotted ALOHA, differently from pure ALOHA, the users are synchronized across time slots of length T_s which is the fixed packet length. G and T definitions change as packets sent per slot and packets cleanly received per slot, respectively. Each user is allowed to send its packets only in the exact time slots. Therefore, a collision occurs only if two or more users send at the same time slot. In Figure 2.2, an example of such a scheme is illustrated. Packets collide in the slots 1 and 5 in which two packets are sent by different users. In the other slots, only one packet is received and there is no interference.

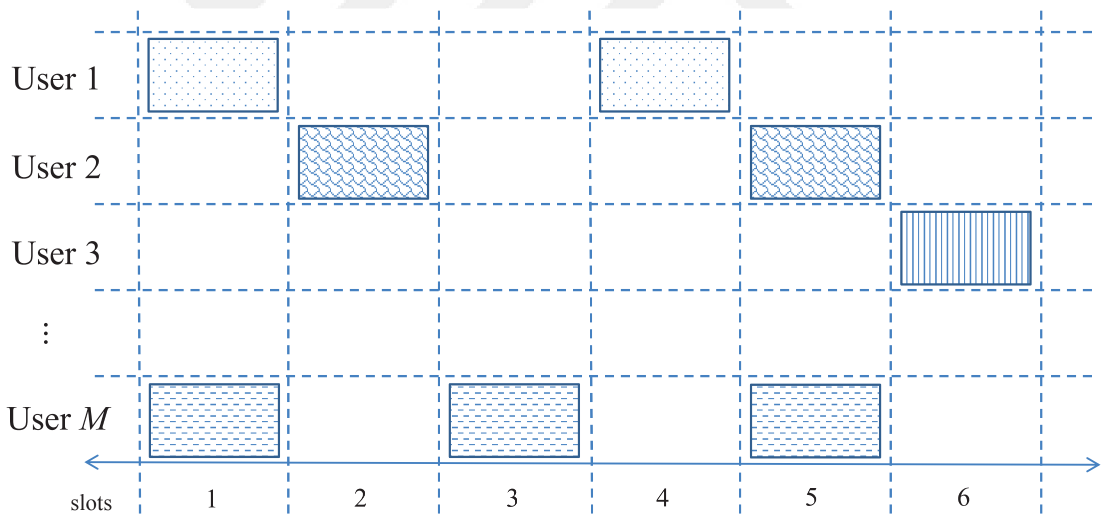

Figure 2.2: The slotted ALOHA scheme from a user-slot perspective.

The number of users sending packets at a given slot is a Poisson random variable. Hence, no collision probability is $\frac{(G)^k e^{-G}}{k!}$ evaluated at $k = 0$ resulting in the probability of no collisions of e^{-G} and the corresponding throughput is $T = Ge^{-G}$. The throughput is maximized at $G = 1$, and the corresponding maximum value is $1/e$.

In Figure 2.3, the resulting throughputs of pure and slotted ALOHA schemes as a function of the offered load are depicted.

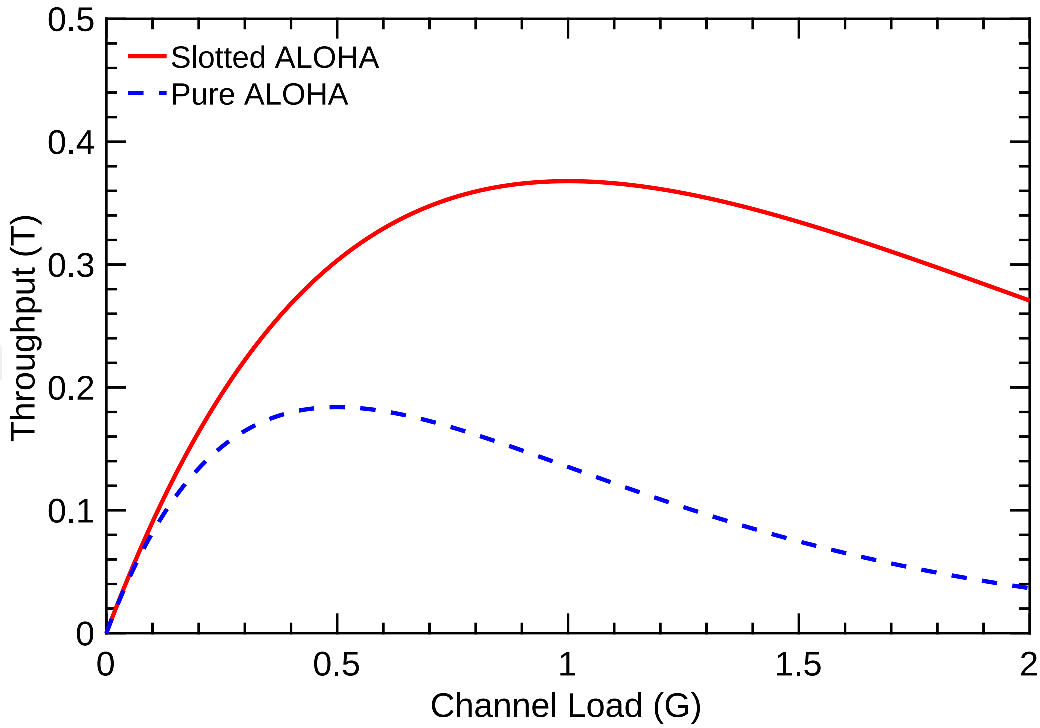

Figure 2.3: Channel load - throughput relationship of pure and slotted ALOHA schemes.

2.3 Irregular Repetition Slotted ALOHA

The utilization of the interference cancellation techniques on the ALOHA-based schemes promise networks supporting high throughput values. In this direction, CRDSA [7] considers grouping a number of slots as frames in which each user sends two copies of its packet by utilizing SIC among different slots to resolve the collisions on the collision channel. Liva generalizes CRDSA and varies the number of copies according to a probability distribution resulting in the scheme is called IRSA [8]. An iterative process to analyze the asymptotic performance of the system for a fixed repetition distribution is also derived in [8]. In this section, IRSA, its convergence analysis, and the asymptotic and finite length simulation results are presented.

2.3.1 System Model

MAC frames of duration T_f are considered. Each frame consists of N slots with duration $T_s = T_f/N$. As in the other slotted ALOHA schemes, each packet is sent in synchrony with the time slots, and packets are considered as bursts. In the analysis, M users are considered where they always send a single packet in each frame, i.e., each user is limited with one transmission attempt either for a new packet or a retransmission. The normalized offered traffic is defined as $G = M/N$ representing the average number of users (packets) per slot. Moreover, the throughput T is defined as the number of successful packet transmissions per slot.

Active users pick a realization of a random variable to select the number of copies of their packets to send using a probability distribution referred to as the RD. In the following, copies of the packets are referred as replicas. At the start of each frame, the users select the slots to send their replicas uniformly and independently of each other. This scheme utilizes the common channel model of RA schemes, namely, the collision channel. Particularly, it is assumed that the receiver is able to recognize the slots with a single replica, collisions and no transmission. The slots with a single replica are always successfully decoded. On the other hand, collisions are considered as non-resolvable, i.e., no information can be obtained from the collision in absence of any additional knowledge. Each packet carries the information of the slots where its copies are sent, and that part of the packet is decoded independently of the whole packet that enables SIC to be employed at the receiver. For SIC, single replicas are resolved. Then, those resolved packets are subtracted from the collisions that include them. This process is iteratively applied until no more messages are resolvable or up to a certain number of iterations.

An example frame of IRSA from a user-slot perspective is given in Figure 2.4. The SIC process employed is very similar to the decoding process of LDPC codes on an erasure channel. Thanks to this similarity, tools from LDPC coding literature can be utilized for analysis and optimization. To do this, first, the

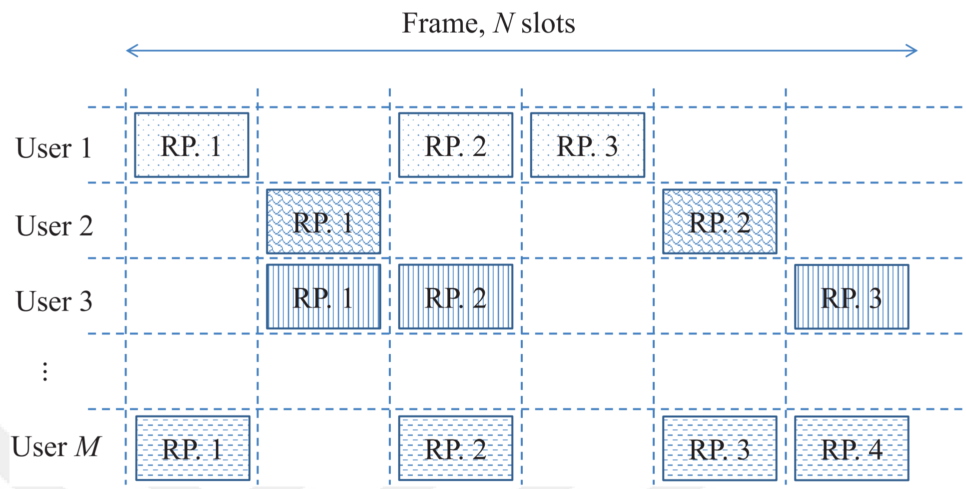

Figure 2.4: IRSA scheme from a user-slot perspective, each user sending repetitions in a frame.

SIC process is represented on a bipartite graph, similar to the Tanner graph representation of LDPC codes. Recall that bipartite graph $\mathcal{G}(B, S, E)$ showing packets and slots connected with edges of repetitions, where B is the set of M burst nodes (BNs) representing the active users, S is the set of N sum nodes (SNs) representing the slots of a frame, and E is the set of edges. An edge connects BN $b_i \in B$ to SN s_j if the ith user sends a replica in the jth slot.

An example of the bipartite graph representation is given in Figure 2.5. The SIC process for the example given in Figure 2.5 is shown in Figure 2.6. In the example, the first node sends its message in the first, second and third slots. Only one replica is received in the third slot which resolves the packet of the first user. It can be seen that, with the iterations of SIC, all the collisions can be resolved for the given example. Through the iterations, the following steps are taken: the first replica of the first packet is obtained from the third slot which carries a single replica. The first packet is subtracted from the collisions on the first and second slots carrying a replica of the packet. Now, the first slot only carries the replica of the second packet, which is then decoded. The second slot which has a collision of the second and third packets is cleaned from the second packet leaving a single replica of the third packet at the second slot. Finally, the third packet which is resolved from the second slot is removed from the fourth slot, and the fourth packet is decoded.

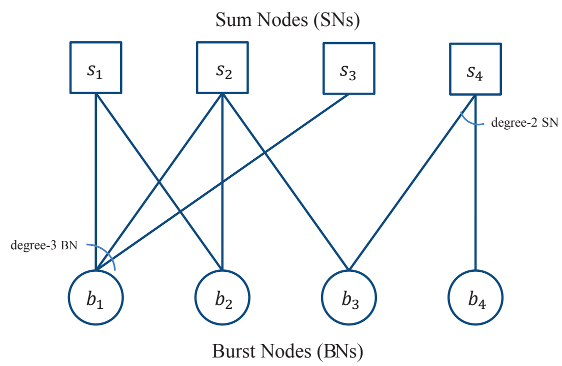

Figure 2.5: Bipartite graph representation of IRSA scheme for an example with 4 users and 4 slots.

Each user draws the number of replicas from a probability distribution denoted by $\{\Lambda_d\}$ which is called as the repetition distribution (RD), e.g., l replicas are sent in a frame with probability Λ_l. For the SNs, the distribution of having l connections (receiving l repetitions) has the probability distribution P_d. These values can be represented via the polynomials

$$\Lambda(x) \triangleq \sum_l \Lambda_l x^l, \quad P(x) \triangleq \sum_l P_l x^l. \tag{2.1}$$

With the definitions in (2.1), the average number of replicas that a user transmits and that is received at a slot become

$$\sum_l l\Lambda_l = \Lambda'(1), \quad \sum_l lP_l = P'(1), \tag{2.2}$$

respectively. Thus, we obtain

$$G = \frac{M}{N} = \frac{P'(1)}{\Lambda'(1)}. \tag{2.3}$$

These equations can also be derived from the edge perspective where λ_l is the probability of an edge being connected to a degree-l BN. In a similar manner, ρ_l is the probability of an edge being connected to a degree-l SN. The polynomial distributions of edge perspective probabilities are defined as

$$\lambda(x) \triangleq \sum_l \lambda_l x^{l-1}, \quad \rho(x) \triangleq \sum_l \rho_l x^{l-1}, \tag{2.4}$$

which can be derived as

$$\lambda_l = \frac{\Lambda_l l}{\sum_l \Lambda_l l}, \quad \rho_l = \frac{P_l l}{\sum_l P_l l}. \tag{2.5}$$

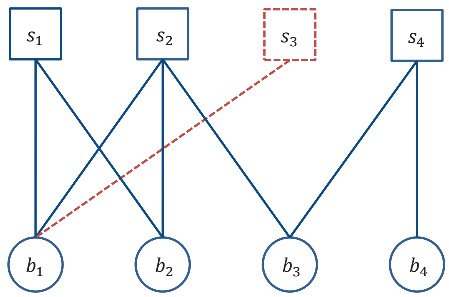

Iteration 1: s_3 is received cleanly.

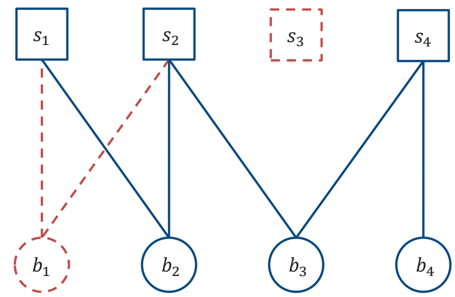

Iteration 2: b_1 is resolved from s_3.

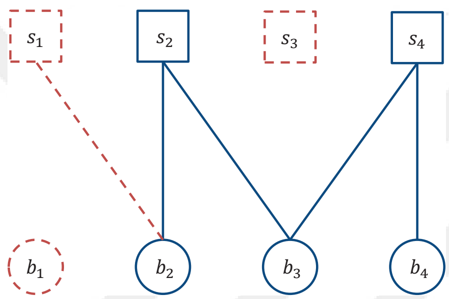

Iteration 3: s_1 and s_2 are cleaned from the replicas of b_1.

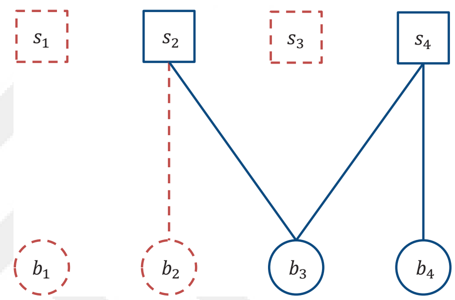

Iteration 4: b_2 is resolved from s_1.

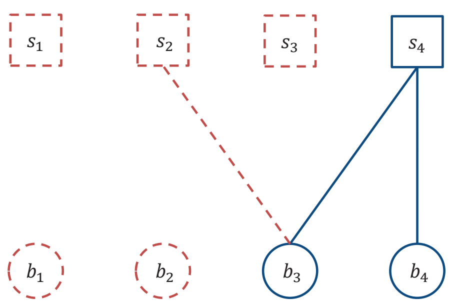

Iteration 5: b_2 is removed from s_2.

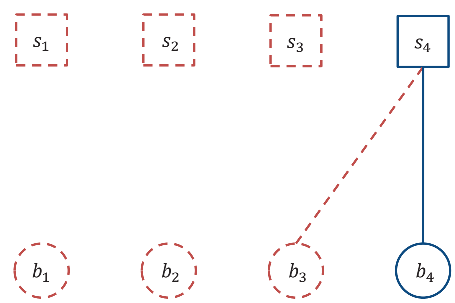

Iteration 6: b_3 is resolved from s_2.

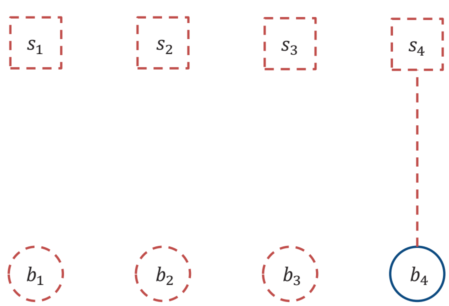

Iteration 7: s_4 is cleaned from b_3.

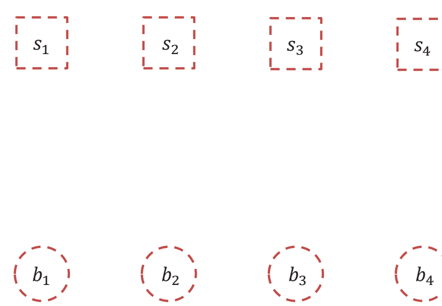

Iteration 8: b_4 is resolved from s_4.

Figure 2.6: The SIC process is represented on a bipartite graph, for an example of 4 users and 4 slots.

2.3.2 Convergence Analysis

With the aim of finding the asymptotic performance of an RD with IRSA, we use a probabilistic approach in which we iterate the average probabilities of edges being not resolved through the SIC iterations in a similar manner with the density evolution of LDPC codes.

Let q and p be the average probabilities of edges connected to SNs and BNs not being resolved, respectively. At the SN side (slots) of SIC, if there is one replica remaining, it can be resolved. Therefore, after the SIC operation at an SN, an edge carries the probability of not being resolved at that iteration depending on the other edges that are connected to the same SN as shown in Figure 2.7. For a degree-l SN, an edge can be revealed if all the other $l-1$ edges connected to that SN are known. Thus, we obtain $p = 1-(1-q)^{l-1}$.

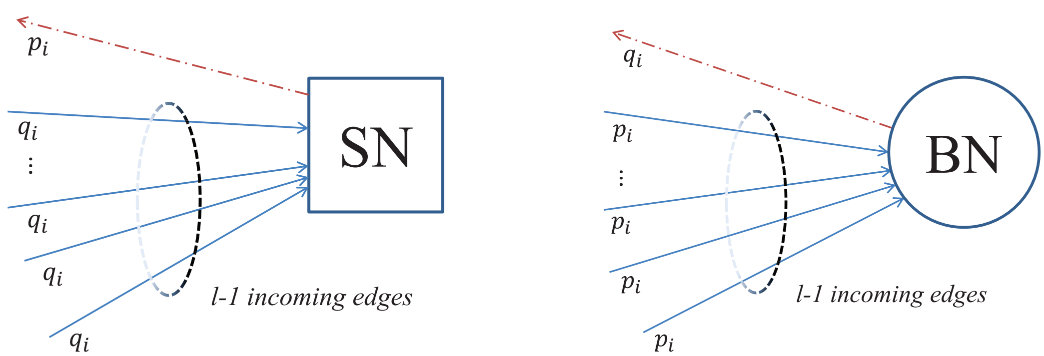

Figure 2.7: A visualization of density evolution probability transfer at degree-l SN and BN, incoming edges carry information to the outgoing edges.

At the BN side (packets) of SIC, if any of the replicas sent is resolved at the last iteration at the SN side, all the replicas of that packet become known. Therefore, from the BN side, the probability of an edge not being resolved is updated as $q = p^{l-1}$.

Since the node degree equations have a varying distribution, we average the update equations over the distributions of the edges, and obtain

$$q_i = \sum_l \lambda_l p_{i-1}^{l-1} = \lambda(p_{i-1}), \tag{2.6}$$

$$p_i = \sum_l \rho_l (1 - (1 - q_i)^{l-1}) = 1 - \rho(1 - q_i), \tag{2.7}$$

where i is the iteration number, q_i is the probability of an edge not being resolved at iteration i after the BN operation, and similarly p_i is the probability of an edge not being resolved at iteration i after the SN operation. At the start of the SIC process, no edge is revealed, thus we initialize $q_0 = p_0 = 1$.

From (2.6) and (2.7), we obtain the iterative update equation as $q_i = \lambda(1 - \rho(1 - q_{i-1}))$. The packet loss ratio (PLR) L_p is defined as the ratio of users whose packets are not resolved, and it is calculated by converting the edge probability to the node probability with $L_p = \Lambda(q_{i_{max}})$, where i_{max} is a sufficiently high number of iterations representing $i_{max} \to \infty$. Below a certain channel load G^*, PLR approaches 0 as the number of iterations goes to ∞ which means that the probability of resolving a packet becomes close to 1. Therefore, G^* can be considered as the maximum asymptotic channel load that can be supported. The system throughput can then be calculated using $T = G(1 - L_p)$. For a sufficiently low PLR, the maximum asymptotic throughput provided by the system T^* is approximately equal to G^*.

To obtain the supported maximum asymptotic channel load G^* with a fixed RD $\Lambda(x)$, the derivation of $\rho(x)$ and $\lambda(x)$ is necessary. $\lambda(x)$ can easily be calculated using a $\Lambda(x)$ by (2.5). As shown in (2.2), the average number of received replicas per slot is $P'(1)$ and they are uniformly distributed. Therefore, a packet is sent in a slot with probability $P'(1)/M$. By noting that the number of edges connected to a slot has a binomial distribution, we write

$$P_l = \binom{M}{l} \left(\frac{P'(1)}{M}\right)^l \left(1 - \frac{P'(1)}{M}\right)^{M-l}, \tag{2.8}$$

and obtain the polynomial function

$$P(x) = \sum_l P_l x^l = \left(1 - \frac{P'(1)(1-x)}{M}\right)^M. \tag{2.9}$$

To be able to utilize the asymptotic probabilistic analysis, we assume infinite number of slots and users. Therefore, using the Poisson approximation of binomials as $M \to \infty$ in (2.9) and changing the variables with those in (2.3), we

Table 2.1: Optimized distributions of IRSA with their channel load thresholds

Distribution, $\Lambda(x)$	G^*
$0.5102x^2 + 0.4898x^4$	0.868
$0.5631x^2 + 0.0436x^3 + 0.3933x^5$	0.898
$0.5465x^2 + 0.1623x^3 + 0.2912x^6$	0.915
$0.5x^2 + 0.28x^3 + 0.22x^8$	0.938
$0.4977x^2 + 0.2207x^3 + 0.0381x^4 + 0.0756x^5 + 0.0398x^6 + 0.0009x^7 +$ $0.0088x^8 + 0.0068x^9 + 0.003x^{11} + 0.0429x^{14} + 0.0081x^{15} + 0.0576x^{16}$	0.965

obtain

$$P(x) = e^{-P'(1)(1-x)} = e^{-G\Lambda'(1)(1-x)}. \tag{2.10}$$

From (2.5), we also have

$$\rho(x) = \frac{P'(x)}{P'(1)} = e^{-G\Lambda'(1)(1-x)}. \tag{2.11}$$

In addition to the derived equations to calculate the PLR and the asymptotic throughput, a differential evolution [9] based search algorithm is utilized to find some optimized RDs providing high G^* values. This is similar to the density evolution of LDPC codes being used to design good codes, hence existing efficient techniques from this literature can be adopted.

2.3.3 Numerical Examples

For the performance evaluation of the IRSA scheme and its convergence analysis, we first optimize the RDs. To do this, we use an evolutionary search algorithm in which the maximum repetition degree is limited to a certain value. As a result, we obtain the RDs providing high channel load thresholds. The optimized distributions of [8] are given in Table 2.1 along with the asymptotic thresholds they offer.

In Figures 2.8 and 2.9, the asymptotic performance of IRSA is determined and it is simulated using the optimized distribution $\Lambda_1 = 0.22x^8 + 0.28x^3 + 0.5x^2$ (with the maximum repetition order 8). In both figures, finite frame length simulations are compared with the theoretical results. In Figure 2.8, the maximum number of iterations is fixed to 100 to observe the effects of the finite frame lengths. First, it can be observed that the finite frame length simulations comply with the asymptotic results, however, depending on the frame length, the maximum throughput provided by the system changes. Having a small number of slots prevents the system from reaching high throughputs, while with a reasonable number of slots (e.g., $N \geq 100$), the simulations show considerably good performance approaching to the asymptotic one.

In Figure 2.9, the effect of maximum number of iterations, i_{max}, is demonstrated. For the number of iterations less than 20, the throughput performance increase considerably with the increase in the number of iterations. On the other hand, for the maximum iterations more than 20, only a slight increase in the performance is obtained. Therefore, the maximum number of iterations of 20 can adopted to keep the complexity of the receiver low without sacrificing almost any system throughput.

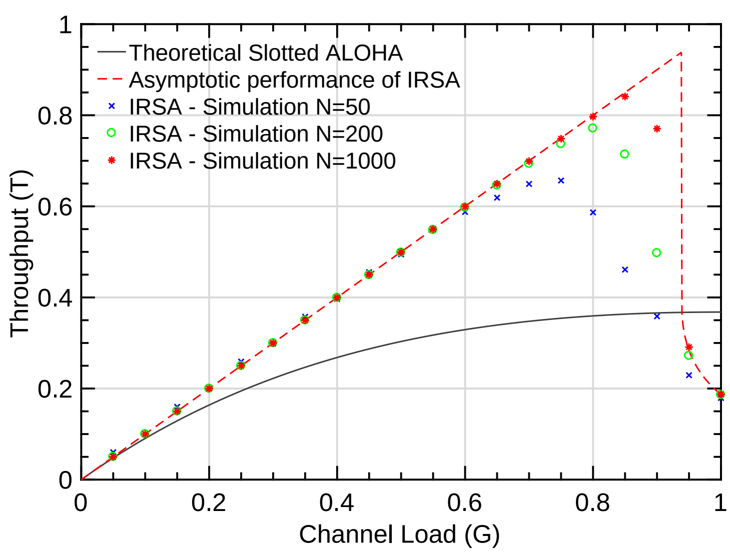

Figure 2.8: Asymptotic performance and finite length simulation results of IRSA with different frame lengths.

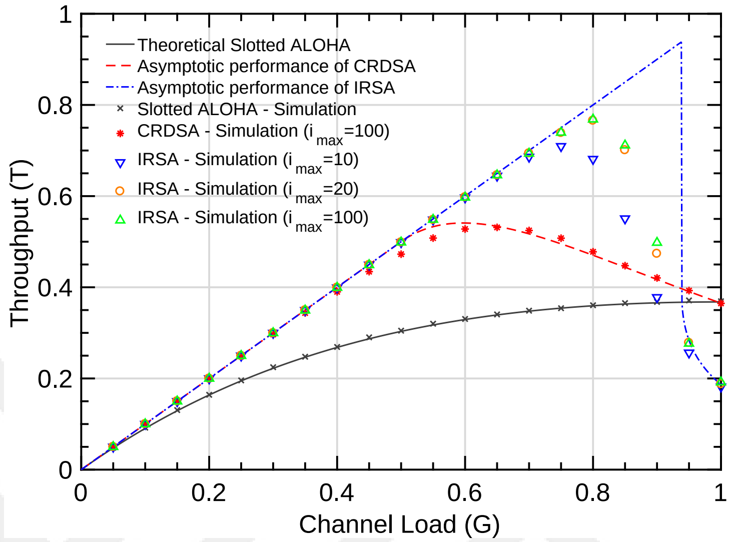

Figure 2.9: Asymptotic performance and finite length simulation results of IRSA with different i_{max} values.

2.4 Chapter Summary

In this chapter, pure and slotted ALOHA schemes are reviewed along with an extensive summary of the model, analysis and numerical results of IRSA. First, pure ALOHA is mathematically described and its throughput performance is demonstrated. Then, the slotted ALOHA scheme is explained with comparisons to pure ALOHA. Finally, the IRSA which is a slotted ALOHA based scheme in which each user sends multiple copies of its packets within each frame is covered. The model, convergence analysis, optimization, and numerical examples of this scheme are given.

Chapter 3

EH-IRSA with Unit Battery Capacity

Studies on MAC protocols including ALOHA variants with MAC nodes are available in many existing papers [23, 26, 30, 32–34]. On the other hand, there is no existing work proposing a CSA based ALOHA scheme providing high throughputs with EH nodes. Given the drastically increasing number of MTDs and their expected lifetime of operation, throughput maximization on uncoordinated RA schemes with EH nodes has a tremendous potential.

In this chapter, we propose a modified IRSA scheme accommodating EH nodes named as energy-harvesting irregular repetition slotted ALOHA (EH-IRSA). In the proposed scheme, sporadically activated users with EH capabilities are equipped with a unit-sized battery where transmission of one packet consumes a unit energy. Users draw the number of replicas for their packets from a probability distribution and select specific time slots to send them across a frame, similar to IRSA. On the other hand, if a user has no energy in its selected slot, transmission cannot take place, hence the allocated slot is skipped. In our model, we assume that the battery is recharged with a certain probability in each slot, independently of the other slots and users. We analyze the asymptotic throughput of the system for a fixed EH rate which is defined as the expected number of energy arrivals in a frame, and we show that finite MAC frame length throughput performances conform with the theoretical (asymptotic) results. Then, we utilize the derived results to find the optimal degree distributions for packet replicas via differential evolution for different EH rates. Our numerical results demonstrate the superiority of the proposed solutions both asymptotically and through extensive finite frame length simulations.

The chapter is organized as follows. In Section 3.1, the system model is given in three parts with the description of the system, energy and channel models. The proposed EH-IRSA scheme is described in Section 3.2. The convergence analysis of the proposed EH-IRSA scheme is presented in Section 3.3. In Section 3.4, several optimized RDs are obtained and their performances are compared with those of CRDSA and IRSA (optimized without the EH considerations), and throughput gain of the proposed solution within the EH framework is demonstrated. The summary of the chapter is provided in Section 3.5.

3.1 System Model

3.1.1 Definitions

We consider a slotted ALOHA scheme in which the time slots are grouped as MAC frames simply referred as frames. Each frame consists of N equal length slots. The number of total users that are sporadically activated (that send messages to the receiver) is denoted by M_t. The users are synchronized across the time slots and frames. Each user is activated with a probability π for a given frame independently of activations in other frames and other users. The number of currently active users is M_a and the channel load of the active users is G_a, while the expected channel load G is defined as the expected number of users per slot given by

$$G_a = \frac{M_a}{N}, \tag{3.1}$$

$$G = \mathbb{E}[G_a] = \frac{\mathbb{E}[M_a]}{N} = \frac{\pi M_t}{N}. \tag{3.2}$$

3.1.2 Energy Model

The transmitting nodes are capable of harvesting energy from a renewable energy source and are equipped with a battery of capacity δ. We assume that transmission of each replica consumes an energy of δ. The batteries of the users are recharged with probability p_c independently in any given time slot if it is not full. We consider $\delta = 1$ for simplicity without any loss in generality. The recharge process is assumed to be an independent and identically distributed Bernoulli process which is a simple model commonly adopted in the literature for EH communication systems [35–38]. The probability of no energy arrival in a particular slot is denoted by $p_{nc} = 1 - p_c$.

Let E_s be the amount of energy at the battery at the start of the s^{th} slot. If a slot is selected for transmission,

$$E_{s+1} = 0$$

since the energy will be consumed. If there is no energy, the slot will be skipped. If the slot s is not selected for transmission, the amount of energy available for the $(s+1)^{th}$ slot is given by

$$E_{s+1} = \begin{cases} 1 & \text{with probability } p_c, \\ E_s & \text{with probability } 1 - p_c. \end{cases}$$

3.1.3 Channel Model

We use the common channel model utilized in the analysis of RA schemes as in [7, 8], the collision channel, and make similar assumptions throughout this chapter. Particularly, we assume that the receiver is able to recognize the slots with single replica, collisions and no transmission. Slots with a single replica are always successfully decoded. On the other hand, collisions are considered as non-resolvable, i.e., no information can be obtained from the collision in absence of any additional knowledge. Each packet carries the information of the slots where its copies are sent and that part of the packet is decoded independently of the whole packet that enables SIC to be employed at the receiver.

3.2 Energy-Harvesting IRSA

In this section, we describe the proposed scheme and analyze its throughput performance. First, the original IRSA is briefly explained. In IRSA [8], each user sends k replicas of its packets with probability Λ_k in any given frame. The probability mass function of the number of replicas sent is represented by the polynomial $\Lambda(x) = \sum_{k=0}^{k_{max}} \Lambda_k x^k$, which is referred to as the RD. The slots in which the replicas are sent are selected uniformly in each frame. The receiver resolves the packets through an iterative process implementing SIC by removing the other copies in different slots of successfully decoded packets.

In the proposed EH-IRSA, the same protocol is adopted along with a modification taking into account the energy state of the battery. A user transmits its replicas during its pre-determined slots only if there is energy stored in its battery, and does not transmit otherwise. In this scheme, although a user may have a certain number of replicas to send, some of these are not transmitted due to the lack of energy. If a node uses an RD of $\Lambda(x)$, due to lack of energy, it will have a different distribution $\tilde{\Lambda}(x)$ corresponding to the probability distribution of the replicas actually being transmitted referred to as the ERD. Replicas which are not sent due to the lack of energy are called as absent replicas (edges), and the rest that are successfully sent are referred to as active replicas (edges).

In Figure 3.1, an example of this scheme is depicted on a bipartite graph. In this example, the number of replicas the users try to send are $\{2, 2, 2, 3\}$. However, they effectively send $\{2, 2, 1, 2\}$ replicas. If this example was reflecting the expected number of packets and energy arrivals, the RD would be $\Lambda_e(x) = \frac{3}{4}x^2 + \frac{1}{4}x^3$ resulting in an ERD of $\tilde{\Lambda}_e(x) = \frac{1}{4}x + \frac{3}{4}x^2$. In Figure 3.2, the same example is shown from a slot-user perspective. If there is no energy arrival after an active replica, then the next replica is absent, i.e., it is not sent due to the lack of energy.

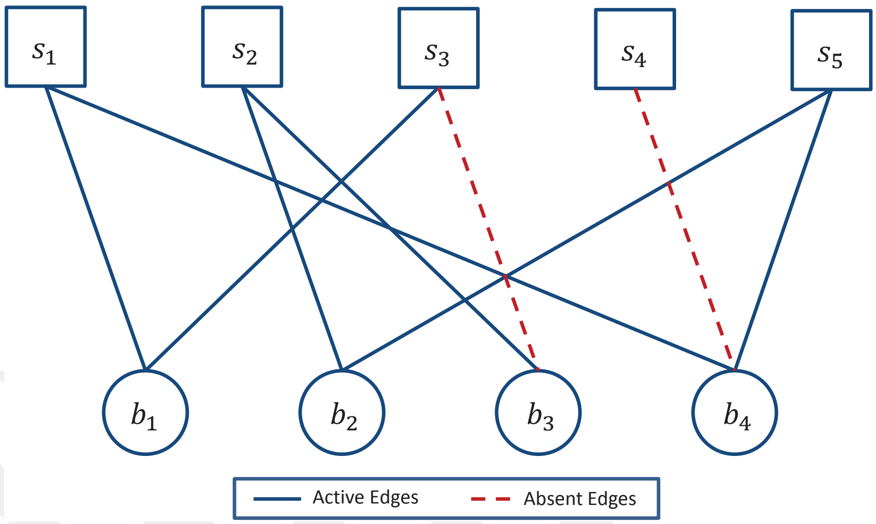

Figure 3.1: An illustration of the proposed scheme with 4 users and 5 slots on a bipartite graph. Burst nodes (circles) represent users and sum nodes (squares) represent slots. Edges connect the users to their pre-determined slots.

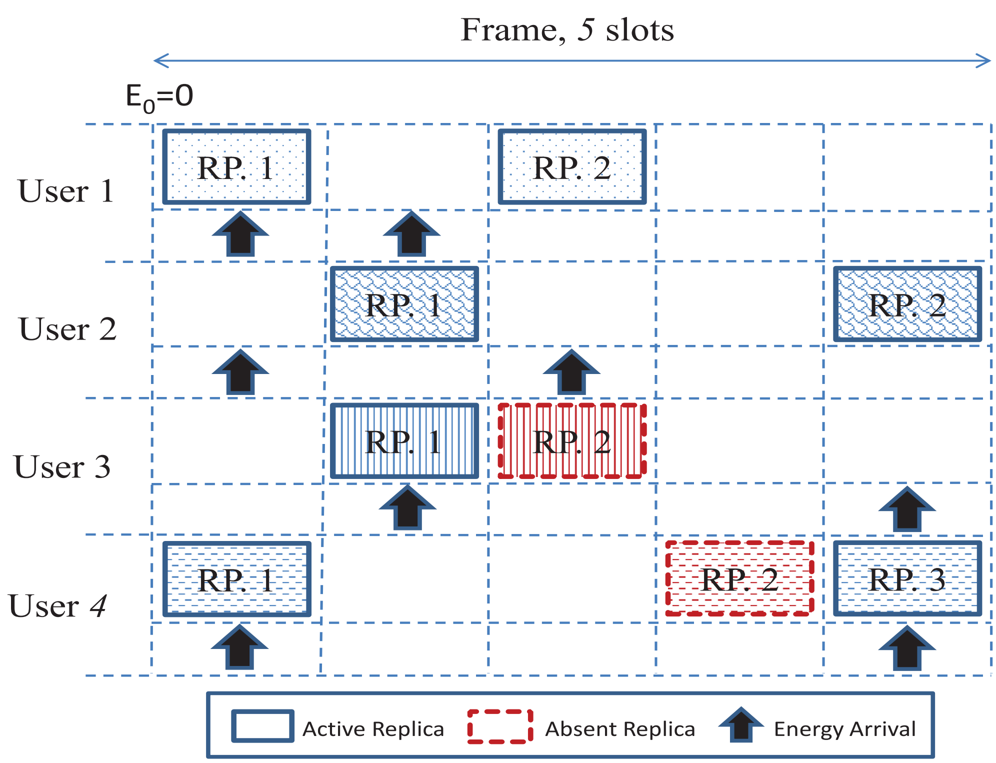

Figure 3.2: The example with 4 users, 5 slots and unit-sized batteries from a slot-user perspective with energy arrivals depicted.

3.3 Convergence Analysis

3.3.1 Density Evolution

Using a similar approach adopted in IRSA, we derive the asymptotic analysis equations to obtain the asymptotic throughput performance of the proposed scheme. We are interested in the asymptotic throughput behavior for a load level G and an EH rate α which is defined as the expected number of energy arrivals in a frame given by $\alpha = Np_c$. We let $M, N \to \infty$ and $p_c \to 0$ while $\alpha = Np_c$ is fixed, and analyze the SIC process from a probabilistic perspective. The density evolution analysis is the same the one with IRSA which is summarized in detail in Chapter 2.

For the performance evaluation, the system throughput is defined as $T = G(1 - L_p)$. For the simulations, we use $G_a = \frac{M_a}{N}$ and L_p which are random variables, and throughput is the expectation of $G_A(1-L_p)$, i.e., $T = E[G_a(1-L_p)]$. By utilizing a differential evolution [9] based optimization algorithm, we obtain RDs that provide the maximum asymptotic channel throughput T^*, we refer this approach to as pure throughput optimization.

We also consider the optimization process to maximize the system throughput while achieving a target PLR. This process is done through a search over the RDs to find the maximum throughput (which is almost equal to the channel load) that provides a target PLR arbitrarily close to 0. This method is referred to as PLR based throughput optimization.

Our main approach is different in the EH scheme since the case in which a user may not be able to send a replica because of no energy arrival before the last selected slot may have a non-negligible probability preventing the PLR L_p going to zero. Moreover, pure throughput optimization forces the PLR to considerably low values since decreasing the PLR and increasing the throughput are have similar effects. This approach results in very close PLR and throughput values for the system specifications when low PLRs can be provided by the PLR based optimization.

To calculate the resulting PLR, we need to derive $\rho(x)$ and $\lambda(x)$ polynomials. To do this, we use the ERDs instead of the RDs in the definitions of the polynomials, and consequently, in the density evolution analysis of the decoding process. To clarify, we only use the active packet replicas, i.e., the absent packet replicas have no effect on the SIC process. Since the absent replicas are ignored in the density evolution analysis, to proceed further we need to calculate the distribution of the active replicas (the ERD).

We further assume that the receiver is able to obtain the knowledge of active and absent edges and it can figure out when a replica was skipped due to the lack of energy. Determining the absent edges is a detection problem that should be considered jointly with the code utilized in the system, and it is beyond the scope of the thesis.

We need to compute the ERD corresponding to a given RD for the analysis of the SIC process, i.e., we need the distributions of the active edges $\tilde{\rho}(x)$ and $\tilde{\lambda}(x)$ which can be calculated using the ERD. Denoting the ERD as

$$\tilde{\Lambda}(x) = \sum_{k=0}^{k_{max}} \tilde{\Lambda}_k x^k, \tag{3.3}$$

we simply change $\Lambda(x)$ to $\tilde{\Lambda}(x)$ in the equations of ρ and λ of IRSA and write

$$\tilde{\lambda}(x) = \frac{\tilde{\Lambda}'(x)}{\tilde{\Lambda}'(1)}, \tag{3.4}$$

$$\tilde{\rho}(x) = e^{-G\tilde{\Lambda}'(1)(1-x)}. \tag{3.5}$$

We assume that the distribution of active replicas is approximately uniform and verify the accuracy of this approximation in the numerical results section by comparing the asymptotic results with finite frame length simulations.

To clarify, in IRSA, the distribution of received packets is a binomial random variable because of the uniformity of the selected slots for sending packets. On the other hand, in EH-IRSA, this is not the case. For instance, clearly the first packet has a different probability than the others due to the sporadic activity of users.

In other words, the users charge their batteries while they are not active which in turn changes the probability of successfully sending the first packet in a frame. Moreover, the other packets are also effected by the recharge process depending on the separation between two consecutively selected packets. However, to make the analysis tractable, we make an approximation. That is, we assume that the probabilities of different packets being transmitted are the same which helps to keep the derivations simple and calculable. This approximation is justified since the distribution of the received packets is uniform for most of the frame excluding the first part, which is shrank by the increasing number of repetitions and the length of the frames.

3.3.2 Effective Repetition Distributions

In this subsection, we compute the ERD for a given RD and EH rate asymptotically as $N, M \to \infty$, $p_c \to 0$ with $\alpha = Np_c$ constant. The additional term $p_c \to 0$ is added to observe the energy harvesting behavior asymptotically. Without that, the distance between two consecutive selected slots goes to ∞ and the probability of being recharged goes to 1. We define Φ_l^k as the probability of having l active replicas out of a total of k active and absent (total) replicas. Also, we define $\Phi^k(x)$ which represents the probability mass function of the number of active replicas when a user selects k replicas to be transmitted in a frame. The resulting ERD and $\Phi^k(x)$ can be written as

$$\tilde{\Lambda}(x) = \sum_{k=0}^{k_{max}} \Lambda_k \Phi^k(x), \tag{3.6}$$

$$\Phi^k(x) = \sum_{l=0}^{k} \Phi_l^k x^l. \tag{3.7}$$

From (3.6) and (3.7), we also have

$$\tilde{\Lambda}_l = \sum_{k=0}^{k_{max}} \Lambda_k \Phi_l^k. \tag{3.8}$$

Due to the sporadic activity of users, the slots after the last transmission trial should be considered. We note that $\Pr\{E_0 = 0\}$ is the probability of not having

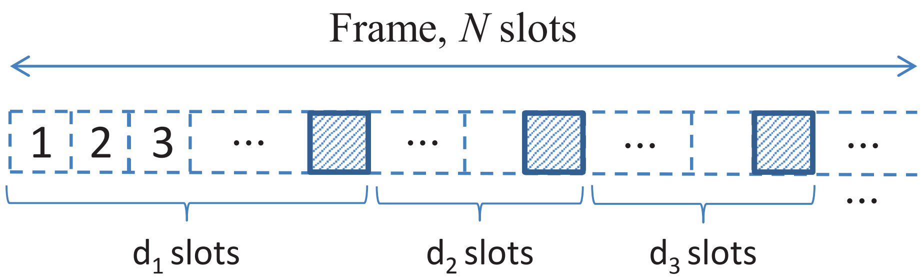

Figure 3.3: A frame of a user is shown with the distance definitions where shaded squares are the selected slots to send replicas.

energy at the beginning of a frame, which depends on the remaining slots after trying to send its last replica in the previous frame for which it is active until the next frame that the user is active again. We denote $\Pr\{E_0 = 1\} = 1 - \Pr\{E_0 = 0\}$ and split Φ_l^k into two parts based on its battery state at the beginning of a frame as

$$\Phi_l^k = \Pr\{E_0 = 1\}\phi_l^k + \Pr\{E_0 = 0\}\bar{\phi}_l^k \tag{3.9}$$

where ϕ_l^k is the probability of l active replicas over k replicas when the first replica is successfully transmitted using the energy at the beginning of the frame, and similarly, $\bar{\phi}_l^k$ is the probability of successful transmission of l replicas over k replicas when the user has no energy at the beginning of the frame.

Let S_i for $i \in [1, k]$ be the random variable indicating that the packet i is active, that is,

$$S_i = \begin{cases} 1 & \text{if the } i\text{th of } k \text{ replicas is active,} \\ 0 & \text{if the } i\text{th of } k \text{ replicas is absent.} \end{cases}$$

To derive ϕ_l^k and $\bar{\phi}_l^k$, we average across the possible k slot selections and l successful transmissions by using the separations among the selected slots denoted by the vector $\boldsymbol{d} = \{d_1, d_2, ..., d_k\}$. This is illustrated in Figure 3.3 on a frame of an active user. Therefore, $\Pr\{S_i = 0\} = p_{nc}^{d_i}$ for $i > 0$ if $E_0 = 0$. If $E_0 = 1$, the first replica is sent, $\Pr\{S_1 = 1\} = 1$ and $\Pr\{S_i = 0\} = p_{nc}^{d_i}$ for $i > 1$. For ease of exposition, we denote summations over all possible distance arrangements from d_1 to d_k over N slots as

$$\sum_{\boldsymbol{d}_1^k} \triangleq \sum_{d_1=1}^{N-k} \sum_{d_2=1}^{N-k+1-d_1} \cdots \sum_{d_{k-1}=1}^{N-\sum_{i=1}^{k-2} d_i - 2} \sum_{d_k=1}^{N-\sum_{i=1}^{k-1} d_i - 1} \tag{3.10}$$

and, we write

$$\begin{aligned}\bar{\phi}_l^k &= \lim_{\substack{N\to\infty\\ p_c\to 0\\ Np_c=\alpha}} \sum_{\forall A_l^k \in \boldsymbol{d}} \sum_{\boldsymbol{d}_1^k} \Pr\{\boldsymbol{d}\} \prod_{i\in\bar{A}_l^k} \Pr\{S_i=0\} \prod_{j\in A_l^k} \Pr\{S_i=1\} \\ &= \lim_{\substack{N\to\infty\\ p_c\to 0\\ Np_c=\alpha}} \sum_{\forall A_l^k \in \boldsymbol{d}} \sum_{\boldsymbol{d}_1^k} \Pr\{\boldsymbol{d}\}\, p_{nc}^{\sum\limits_{i\in\bar{A}_l^k} d_i} \prod_{j\in A_l^k} (1-p_{nc}^{d_j}),\end{aligned} \tag{3.11}$$

where $\bar{A}_l^k$ is the set of indices of the distances before the $k-l$ absent replicas, A_l^k is the set of indices of the distances before the l active replicas and $\Pr\{\boldsymbol{d}\}$ is the probability of the specific selection of the slots which is the same for all selections, $1/\binom{N}{k}$. Note that $A_l^k \cup \bar{A}_l^k = \boldsymbol{d}$. Also, the set of summations $\sum_{\boldsymbol{d}_1^k}$ is symmetric for each element of $\boldsymbol{d}$. In other words, without changing the function inside $\sum_{\boldsymbol{d}_1^k}$ any d_i and d_j for each i,j can be interchanged in the right hand side of (3.10). The first summation in (3.11) is over all the possible l active slot selections out of k total slots. It is clear that, for any possible selection of A_l^k, $\sum_{\boldsymbol{d}_1^k}^N$ is the same since the probabilities of all the possible arrangements $\Pr\{\boldsymbol{d}\}$ are the same and the summation $\sum_{d_1^k}$ is for all possible distance arrangements of all the replicas and it is symmetric. Hence, we obtain

$$\bar{\phi}_l^k = \lim_{\substack{N\to\infty\\ p_c\to 0\\ Np_c=\alpha}} \frac{\binom{k}{l}}{\binom{N}{k}} \sum_{\boldsymbol{d}_1^k} p_{nc}^{\sum_{i=l+1}^k d_i} \prod_{j=1}^{l} (1-p_{nc}^{d_j}). \tag{3.12}$$

The multiplication of charging probabilities inside $\sum_{\boldsymbol{d}_1^k}$ can be written as a sum of various powers of p_{nc}. These powers are summations of some of the distances d_i's. We also note that if the number of distances in the power of p_{nc} are the same, they give equal value inside the summation $\sum_{\boldsymbol{d}_1^k}$. Therefore, we can modify (3.12) further, by using the symmetry of the distances of all possible distance arrangements and write

$$\bar{\phi}_l^k = \lim_{\substack{N\to\infty\\ p_c\to 0\\ Np_c=\alpha}} \frac{\binom{k}{l}}{\binom{N}{k}} \sum_{\boldsymbol{d}_1^k} p_{nc}^{\sum_{i=l+1}^k d_i} \sum_{r=0}^{l} (-1)^r \binom{l}{r} p_{nc}^{\sum_{i=1}^r d_i}. \tag{3.13}$$

Defining

$$f(k,r) \triangleq \lim_{\substack{N\to\infty\\ p_c\to 0\\ Np_c=\alpha}} \frac{1}{\binom{N}{k}} \sum_{\boldsymbol{d}_1^k} p_{nc}^{\sum_{i=1}^r d_i}, \tag{3.14}$$

and by using (3.13) and (3.14), we can write

$$\bar{\phi}_l^k = \binom{k}{l} \sum_{r=0}^{l} \binom{l}{r} (-1)^r f(k, k-l+r), \tag{3.15}$$

which is in a simple form in terms of the f function defined in (3.14). We can numerically calculate $f(k,r)$ for all possible k, r values, and we can compute any $\bar{\phi}_l^k$ of ERD from the given RD. Moreover, the complexity of the numerical calculations can be decreased with the following recursive relations whose proofs are given below:

$$-\frac{df(k,r)}{d\alpha}\frac{k+1}{r} = f(k+1, r+1), \tag{3.16}$$

$$\left(\frac{df(k,r)}{d\alpha} + f(k,r)\right)\frac{k+1}{k+1-r} = f(k+1, r), \tag{3.17}$$

$$f(1,1) = \frac{1-e^{-a}}{\alpha}, \quad k, r \geq 1. \tag{3.18}$$

Note that (3.15)-(3.18) provide a feasible and simple method to compute $\bar{\phi}_l^k$ for a given RD and an EH rate α.

To prove the relationship in (3.16), we start with the definition in (3.14). The function $f(k,r)$ can be written in a different form as follows:

$$\begin{aligned} f(k,r) &\triangleq \lim_{\substack{N\to\infty \\ p_c\to 0 \\ Np_c=\alpha}} \frac{1}{\binom{N}{k}} \sum_{\boldsymbol{d}_1^k}^{N} p_{nc}^{\sum_{i=1}^{r} d_i} \\ &= \lim_{\substack{N\to\infty \\ p_c\to 0 \\ Np_c=\alpha}} \frac{1}{\binom{N}{k}} \sum_{i=r}^{N-k+r} \binom{i-1}{r-1}\binom{N-i}{k-r} p_{nc}^{i}. \end{aligned} \tag{3.19}$$

We take the derivative of $f(k,r)$ with respect to p_{nc}, and obtain

$$\frac{df(k,r)}{dp_{nc}}\frac{k+1}{r} = \lim_{\substack{N\to\infty \\ p_c\to 0 \\ Np_c=\alpha}} \frac{N}{\binom{N}{k+1}} \sum_{i=r}^{N-k+r} \binom{i}{r}\binom{N-i}{k-r} p_{nc}^{i-1}.$$

We note that $d\alpha = -Ndp_{nc}$, and find the derivative with respect to α by a change of variables,

$$-\frac{df(k,r)}{d\alpha}\frac{k+1}{r} = \lim_{\substack{N\to\infty \\ p_c\to 0 \\ Np_c=\alpha}} \frac{1}{\binom{N}{k+1}} \sum_{i=r}^{N-k+r} \binom{i}{r}\binom{N-i}{k-r} p_{nc}^{i-1}. \tag{3.20}$$

By changing the limits of the summation from $(r,N-k+r)$ to $(r+1,N-k+r+1)$ we get

$$-\frac{df(k,r)}{d\alpha}\frac{k+1}{r}=\lim_{\substack{N\to\infty\\p_c\to 0\\Np_c=\alpha}}\frac{1}{\binom{N}{k+1}}\sum_{i=r+1}^{N-k+r+1}\binom{i-1}{r}\binom{N-i+1}{k-r}p_{nc}^{i-2},$$

and we decrement each N inside the limit by 1, since the final results is not affected considering the limit $N\to\infty$, i.e.,

$$\begin{aligned}-\frac{df(k,r)}{d\alpha}\frac{k+1}{r}&=\lim_{\substack{N\to\infty\\p_c\to 0\\Np_c=\alpha}}\frac{1}{\binom{N-1}{k+1}}\sum_{i=r+1}^{N-k+r}\binom{i-1}{r}\binom{N-i}{k-r}p_{nc}^{i-2}\\&=\lim_{\substack{N\to\infty\\p_c\to 0\\Np_c=\alpha}}\frac{1}{\binom{N}{k+1}}\sum_{i=r+1}^{N-k+r}\binom{i-1}{r}\binom{N-i}{k-r}p_{nc}^{i}\\&=f(k+1,r+1),\end{aligned}$$

concluding the proof of (3.16).

The relationship in (3.17) can be proved starting with (3.19). We have

$$f(k,r)=\lim_{\substack{N\to\infty\\p_c\to 0\\Np_c=\alpha}}\frac{1}{\binom{N}{k}}\sum_{i=r}^{N-k+r}\binom{i-1}{r-1}\binom{N-i}{k-r}p_{nc}^{i}.$$

By changing the parameter N inside the limit with $N-1$, we obtain

$$\begin{aligned}f(k,r)&=\lim_{\substack{N\to\infty\\p_c\to 0\\Np_c=\alpha}}\frac{1}{\binom{N}{k}}\sum_{i=r}^{N-k+r-1}\binom{i-1}{r-1}\binom{N-i-1}{k-r}p_{nc}^{i}\\&=\lim_{\substack{N\to\infty\\p_c\to 0\\Np_c=\alpha}}\frac{1}{\binom{N}{k}}\sum_{i=r}^{N-k+r-1}\frac{k-r+1}{N-i}\binom{i-1}{r-1}\binom{N-i}{k-r+1}p_{nc}^{i},\\&=\lim_{\substack{N\to\infty\\p_c\to 0\\Np_c=\alpha}}\frac{N}{k+1}\frac{1}{\binom{N}{k+1}}\sum_{i=r}^{N-k+r-1}\frac{k-r+1}{N-i}\binom{i-1}{r-1}\binom{N-i}{k-r+1}p_{nc}^{i},\end{aligned}$$

From (3.20) we also have

$$\frac{df(k,r)}{d\alpha}=\lim_{\substack{N\to\infty\\p_c\to 0\\Np_c=\alpha}}-\frac{r}{k+1}\frac{1}{\binom{N}{k+1}}\sum_{i=r}^{N-k+r}\binom{i}{r}\binom{N-i}{k-r}p_{nc}^{i-1}.$$

Similarly, by changing Ns inside the limit with $N-1$, we obtain

$$\begin{aligned}
\frac{df(k,r)}{d\alpha} &= \lim_{\substack{N\to\infty\\ p_c\to 0\\ Np_c=\alpha}} -\frac{r}{k+1}\frac{1}{\binom{N}{k+1}}\sum_{i=r}^{N-k+r-1}\binom{i}{r}\binom{N-i-1}{k-r}p_{nc}^{i-1}\\
&= \lim_{\substack{N\to\infty\\ p_c\to 0\\ Np_c=\alpha}} -\frac{1}{k+1}\frac{1}{\binom{N}{k+1}}\sum_{i=r}^{N-k+r-1}\frac{i(k-r+1)}{N-i}\binom{i-1}{r-1}\binom{N-i}{k-r+1}p_{nc}^{i}.
\end{aligned}$$

Therefore, we can write

$$f(k,r)+\frac{df(k,r)}{d\alpha} = \lim_{\substack{N\to\infty\\ p_c\to 0\\ Np_c=\alpha}} \frac{k-r+1}{k+1}\frac{1}{\binom{N}{k+1}}\sum_{i=r}^{N-k+r-1}\frac{N-i}{N-i}\binom{i-1}{r-1}\binom{N-i}{k-r+1}p_{nc}^{i},$$

and we finally obtain

$$\begin{aligned}
\left(\frac{df(k,r)}{d\alpha}+f(k,r)\right)\frac{k+1}{k+1-r} &= \lim_{\substack{N\to\infty\\ p_c\to 0\\ Np_c=\alpha}} \frac{1}{\binom{N}{k+1}}\sum_{i=r}^{N-k+r-1}\binom{i-1}{r-1}\binom{N-i}{k-r+1}p_{nc}^{i},\\
&= f(k+1,r),
\end{aligned}$$

which is the desired result.

Finally, in order to derive (3.18) we proceed as follows. Using the definition in (3.14), we simply set $k=1$, $r=1$, and apply the sum of power series

$$\begin{aligned}
f(1,1) &= \lim_{\substack{N\to\infty\\ p_c\to 0\\ Np_c=\alpha}} \frac{1}{N}\sum_{d_1=1}^{N}p_{nc}^{d_1}\\
&= \lim_{\substack{N\to\infty\\ p_c\to 0\\ Np_c=\alpha}} \frac{1}{N}\frac{p_{nc}-p_{nc}^{N+1}}{1-p_{nc}}\\
&= \lim_{\substack{N\to\infty\\ p_c\to 0\\ Np_c=\alpha}} \frac{p_{nc}-p_{nc}^{N+1}}{Np_c}\\
&= \frac{1-\lim(1-\frac{\alpha}{N})^{N+1}}{\alpha}\\
&= \frac{1-e^{-\alpha}}{\alpha}.
\end{aligned}$$

For the case with energy at the beginning of the frame, we consider $\tilde{k}=k-1$ and $\tilde{l}=l-1$ ignoring the first replica that is sent all the time since battery is charged at the start of the frame, $\Pr\{S_1 = 1\} = 1$. Thus, in a complementary manner to (3.12) through (3.15), we obtain

$$
\begin{aligned}
\phi_l^k &= \lim_{\substack{N\to\infty \\ p_c\to 0 \\ Np_c=\alpha}} \frac{\binom{\tilde{k}}{\tilde{l}}}{\binom{N}{k}} \sum_{\boldsymbol{d}_1^k} p_{nc}^{\sum_{i=l+1}^{k} d_i} \prod_{j=2}^{l} (1 - p_{nc}^{d_j}), \\
&= \binom{\tilde{k}}{\tilde{l}} \sum_{r=0}^{\tilde{l}} \binom{\tilde{l}}{r} (-1)^r f(k, k-l+r),
\end{aligned} \tag{3.21}
$$

concluding the derivation.

To sum up, we can compute the ERDs corresponding to any given RD and any EH rate α which can be used to obtain the asymptotic throughput performance of the system.

We also note that the probability of the energy states before the first slot of a frame $\Pr\{E_0 = 0\}$ and $\Pr\{E_0 = 1\}$ are also needed. Recall that, $\Pr\{E_0 = 1\}$ was defined as the average probability of having energy at the start of a frame and since the battery is unit-sized, $\Pr\{E_0 = 1\} = 1 - \Pr\{E_0 = 0\}$. We use these terms in our asymptotic analysis, therefore they are computed under the same (asymptotic) assumptions.

$\Pr\{E_0 = 1\}$ depends on two different variables: the last slot that a user tries to send a replica and the number of frames between two consecutive frames that the user is active. We denote the expected probability of not being charged after the last trial of sending the replica in that frame as P'_{slots} and the expected probability of being not charged during the frames that user is not active as P'_{frames}. We can write

$$
\Pr\{E_0 = 0\} = P'_{slots} P'_{frames}. \tag{3.22}
$$

as these two events are independent.

We form P'_{slots} as

$$
P'_{slots} = \lim_{\substack{N\to\infty \\ p_c\to 0 \\ Np_c=\alpha}} \sum_{k=1}^{k_{max}} \Lambda_k \sum_{i=1}^{N-k+1} \binom{N-i}{k-1} p_{nc}^{i}, \tag{3.23}
$$

which is the expected probability of not being charged after the last trial of transmission with the averaging over the RD. The number of possible ways of selecting the i-th slot from the end of a frame as the last slot for a replica is $\binom{N-i}{k-1}$. Then, we note that the inner summation is equivalent to $f(k,1)$, and we simplify the expression as

$$P'_{slots} = \sum_{k=1}^{k_{max}} \Lambda_k f(k,1). \tag{3.24}$$

The effect of the frames between the consecutive frames that a user is active can be expressed as the probability of no energy arrival in those frames, i.e.,

$$\begin{aligned} P'_{frames} &= \lim_{\substack{N\to\infty \\ p_c\to 0 \\ Np_c=\alpha}} \pi p_{nc}^0 + \pi(1-\pi)p_{nc}^N + \pi(1-pi)^2 p_{nc}^{2N} + \dots \\ &= \lim_{\substack{N\to\infty \\ p_c\to 0 \\ Np_c=\alpha}} \pi \sum_{i=0}^{\infty} [(1-\pi)p_{nc}^N]^i \\ &= \lim_{\substack{N\to\infty \\ p_c\to 0 \\ Np_c=\alpha}} \frac{\pi}{1-(1-\pi)p_{nc}^N} \\ &= \frac{\pi}{1-(1-\pi)e^{-\alpha}}. \end{aligned} \tag{3.25}$$

Finally, combining (3.22), (3.24) and (3.25), we obtain

$$\Pr\{E_0 = 0\} = \frac{\pi}{1-(1-\pi)e^{-\alpha}} \sum_{k=1}^{k_{max}} \Lambda_k f(k,1). \tag{3.26}$$

3.4 Numerical Examples

In this section, we present several numerical examples to illustrate the results of our asymptotic analysis along with the simulations of the EH-IRSA scheme. First, for fixed α and π values, we search for RDs providing the largest T^* values via differential evolution using the proposed convergence analysis. For the search, we limit the maximum repetition degree to 8. For the finite length simulations,

Table 3.1: EH-IRSA the optimized RDs and the corresponding ERDs for $\alpha = 2, 5, 8$, $\pi = 0.1, 1$ and $B = 1$.

$\boldsymbol{\alpha}$	$\boldsymbol{\pi}$	**Repetition Distribution, $\boldsymbol{\Lambda(x)}$** **Effective Repetition Distribution, $\boldsymbol{\widetilde{\Lambda}(x\mid\pi,\alpha)}$**	$\boldsymbol{T^*}$
2	1	$\Lambda_{max}(x) = x^8$ $\widetilde{\Lambda}_{max}(x) = 0.14x^1 + 0.34x^2 + 0.32x^3 + 0.15x^4 + 0.04x^5 + 0.01x^6$	0.5105
5	0.1	$\Lambda_1(x) = 0.25x^3 + 0.13x^7 + 0.62x^8$ $\widetilde{\Lambda}_1(x) = 0.06x^2 + 0.25x^3 + 0.32x^4 + 0.22x^5 + 0.11x^6 + 0.03x^7 + 0.01x^8$	0.8700
		$\Lambda_L(x) = 0.5x^2 + 0.28x^3 + 0.22x^8$ $\widetilde{\Lambda}_L(x) = 0.21x^2 + 0.52x^3 + 0.16x^4 + 0.07x^5 + 0.03x^6 + 0.01x^7$	0.5791
		$\Lambda_C(x) = x^2$ $\widetilde{\Lambda}_C(x) = 0.33x^2 + 0.67x^3$	0.4633
	1	$\Lambda_2(x) = 0.02x^4 + 0.02x^5 + 0.34x^7 + 0.62x^8$ $\widetilde{\Lambda}_2(x) = 0.01x^1 + 0.08x^2 + 0.23x^3 + 0.32x^4 + 0.24x^5 + 0.10x^6 + 0.02x^7$	0.8682
		$\Lambda_L(x)$ $\widetilde{\Lambda}_L(x) = 0.02x^1 + 0.27x^2 + 0.47x^3 + 0.14x^4 + 0.06x^5 + 0.03x^6 + 0.01x^7$	0.5518
		$\Lambda_C(x)$ $\widetilde{\Lambda}_C(x) = 0.03x^1 + 0.37x^2 + 0.60x^3$	0.4541
8	1	$\Lambda_3(x) = 0.28x^2 + 0.08x^4 + 0.06x^5 + 0.07x^6 + 0.51x^8$ $\widetilde{\Lambda}_3(x) = 0.09x^2 + 0.28x^3 + 0.19x^4 + 0.22x^5 + 0.15x^6 + 0.06x^7 + 0.01x^8$	0.8743

we normalize the number of total users M_t to change the expected load G while keeping the activity probability π and number of slots N the same.

As examples, some maximum asymptotic throughputs of the optimized distributions for $\alpha = 2, 5, 8$ and $\pi = 0.1, 1$ are presented in Table 3.1 along with the corresponding ERDs for the given α and π values. $\Lambda_L(x)$ is the 8-th order optimized distribution of IRSA in [8] and $\Lambda_C(x)$ is the regular order-2 distribution of CRDSA. Although the optimized RDs have the high probability of the maximum repetition number selected, this probability is very low in the corresponding

ERDs which shows that the optimization process has a tendency towards to increasing the probability of higher order repetitions of the RDs to remedy the unpredictability of the energy arrivals.

In Figures 3.4 and 3.5, we present our results on the resulting throughput as a function of G for the cases with activity probabilities $\pi = 0.1$ and $\pi = 1$ respectively with an EH rate $\alpha = 5$, and a frame length $N = 300$. In the both given cases, the maximum throughput provided by $\Lambda_L(x)$ is about 0.57 while the newly optimized distributions $\Lambda_1(x)$ and $\Lambda_2(x)$ can offer a maximum asymptotic throughput of 0.87 which is a substantial gain. Moreover, the finite length simulation results conform with the throughputs obtained with the asymptotic analysis hence they verify the accuracy of the uniformity approximation used in the asymptotic analysis. In Figure 3.6, the PLR and throughput graphs for the case $\pi = 1$ while $\alpha = 2$ is given. From the given figures, we observe that the analysis fits very tightly for the case of full activity $\pi = 1$ independent of the EH rate. However, for $\pi = 0.1$, there is a small gap in Figure 3.4 which may be caused from the uniformity approximation of the active packets.

To illustrate the system performance further with different energy harvesting rates, we provide Figure 3.7 which depicts the maximum throughputs of the newly optimized distributions with all users being active ($\pi = 1$) as a function of α. The results show that by using the EH rate in the optimization we can achieve higher throughputs compared to the other distributions. Figure 3.7 also shows that $\Lambda_L(x)$ requires a much higher value of α to approach the optimized distribution of the system noting that for the values of α that approach N, the EH nodes have energy (almost) all the time and the IRSA optimization works well.

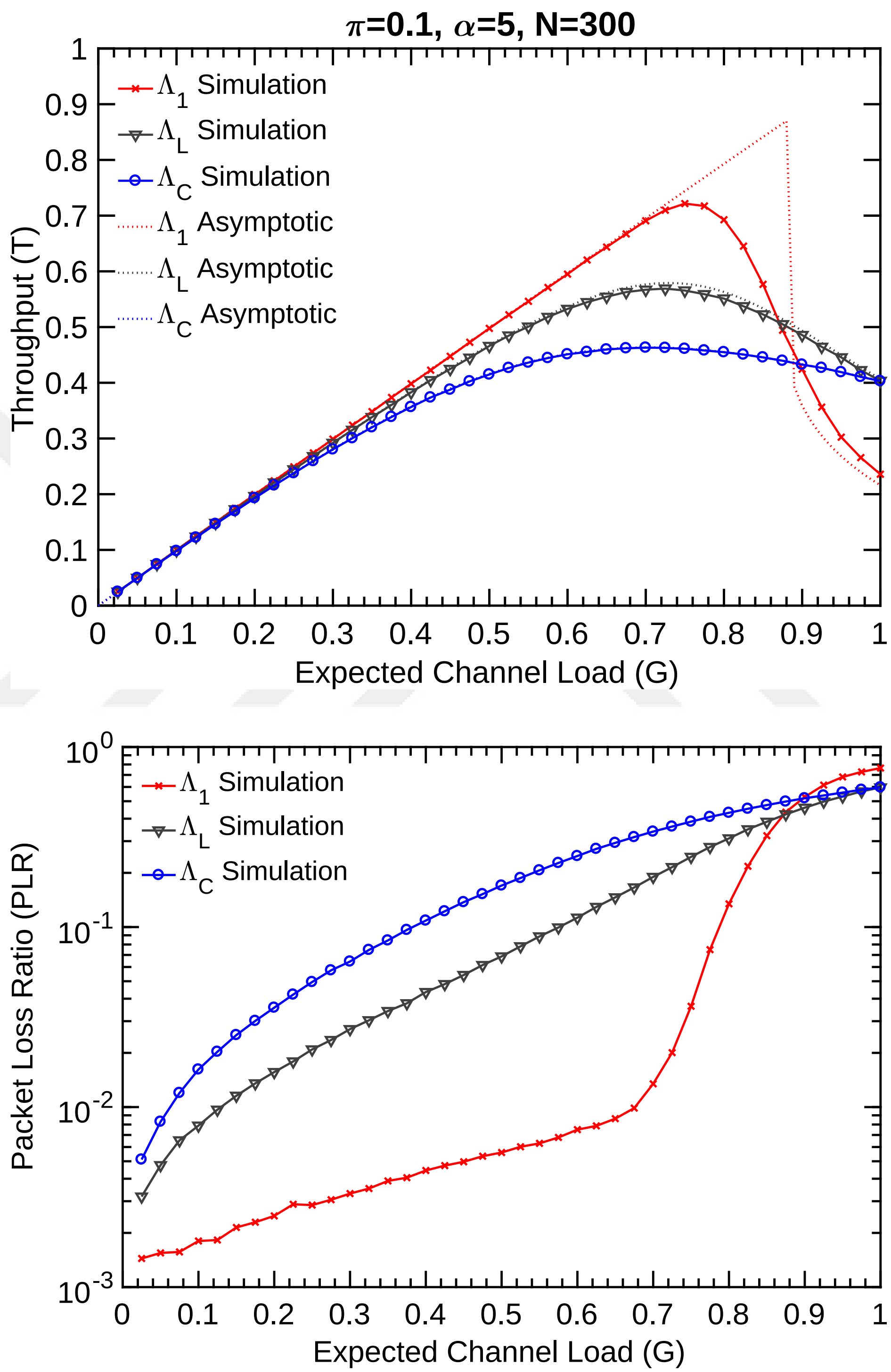

Figure 3.4: The results of the simulation and analysis for an energy harvesting rate of 5, a frame length of 300 and an activity probability of 0.1 with a unit-sized battery ($B = 1$).

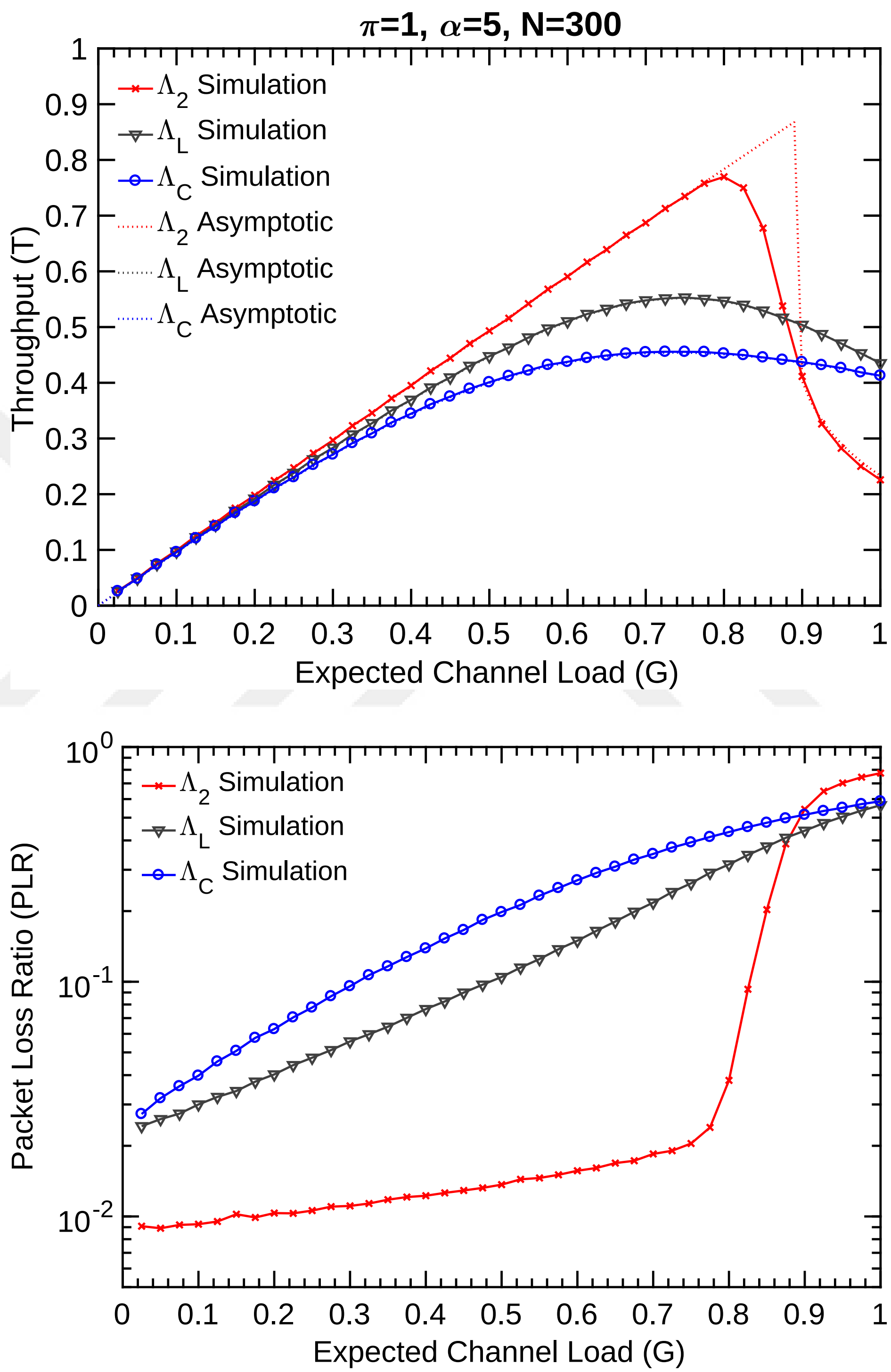

Figure 3.5: The results of the simulation and analysis for an energy harvesting rate of 5, a frame length of 300 and an activity probability of 1 with a unit-sized battery ($B = 1$).

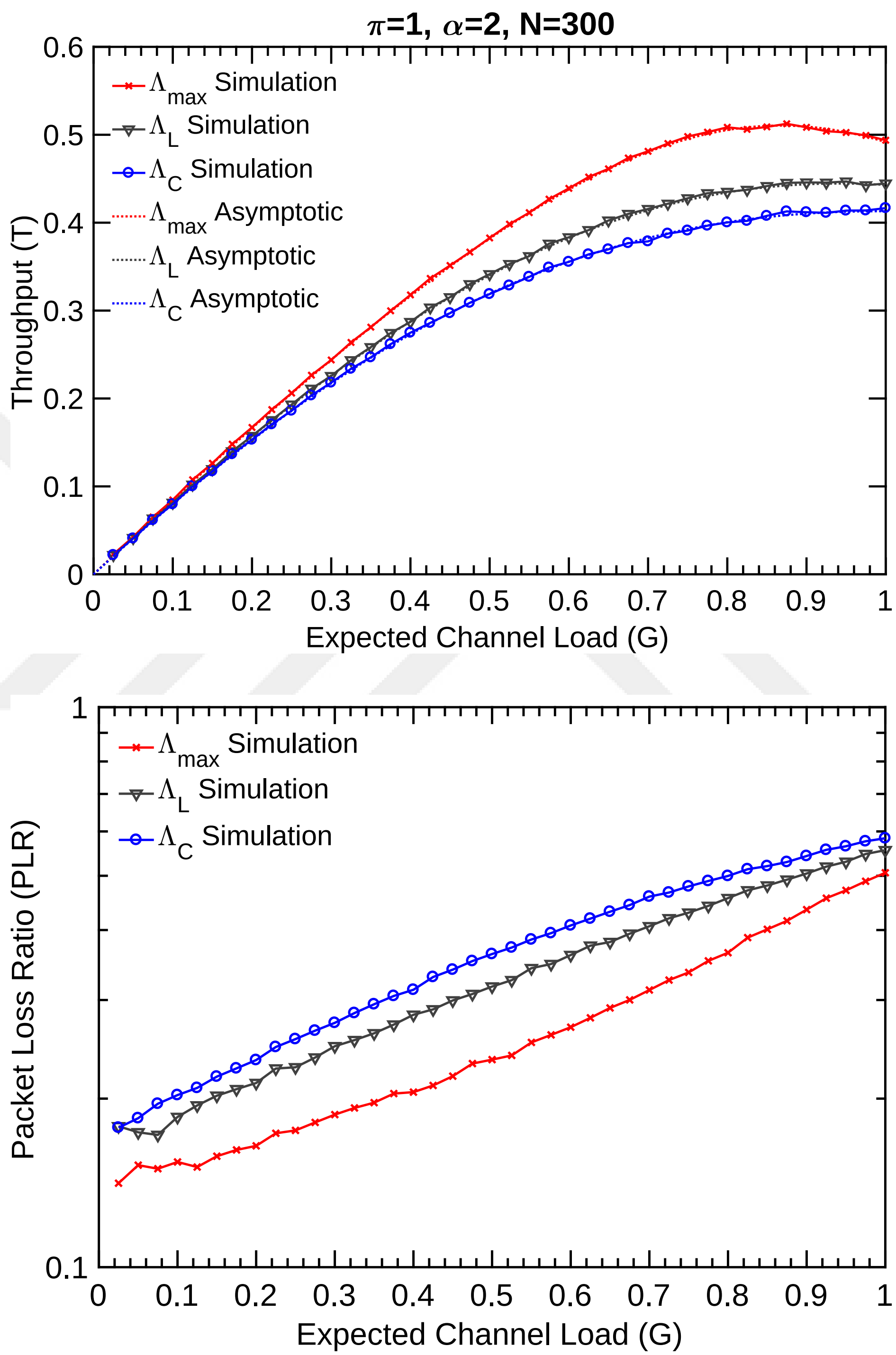

Figure 3.6: The results of the simulation and analysis for an energy harvesting rate of 2, a frame length of 300 and an activity probability of 1 with a unit-sized battery ($B = 1$).

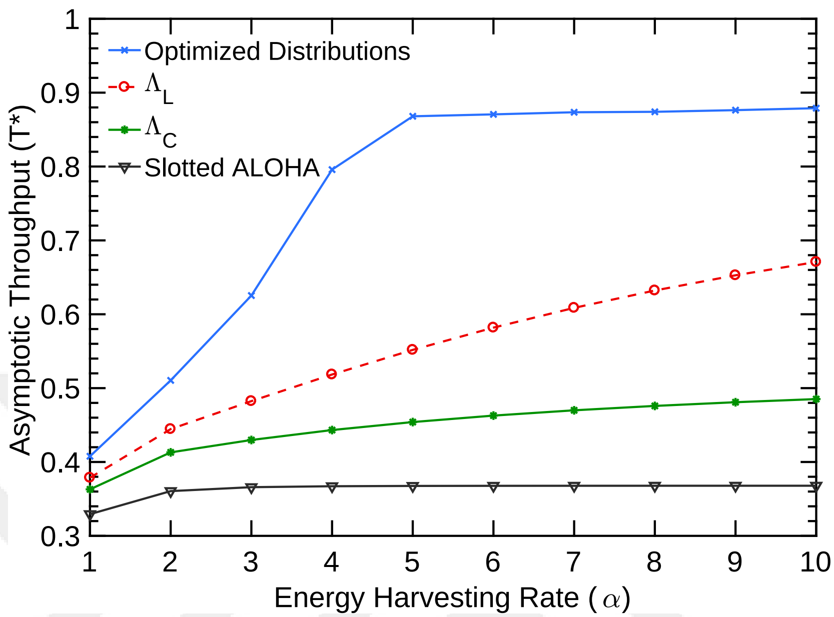

Figure 3.7: Comparison of the resulting asymptotic throughput of the pure throughput based optimized distributions for different EH rates with an activity probability of 1.

Up to this point, we have only considered the pure throughput based optimization. Next, we consider a PLR based optimization where the aim is to find maximum asymptotic channel load G^* providing a certain target PLR. Figures 3.8 and 3.9 illustrate the target PLR of 3.10^{-2} and 10^{-2} based channel load optimization results, respectively. From Figures 3.7, 3.8 and 3.9, we conclude that if the energy arrival rate is sufficiently high (e.g., $\alpha \geq 5$), the maximum throughput and channel load reaches a high value for both optimization cases. Above some critical value of α, the RD optimization providing a target PLR results in a high asymptotic channel load. This critical value slightly changes with different target values of the PLR. Below this critical value where the target PLR is not achievable, the all the optimizations result in the maximum degree repetition distribution $\Lambda_{max} = x^8$ which is the trivial solution where the users send their repetitions as soon as possible when the energy arrival is scarce. This can also be seen from Figure 3.6 with $\alpha = 2$ case in more detail. Below the threshold EH rate, the PLR based optimization results in a near zero achievable channel load.

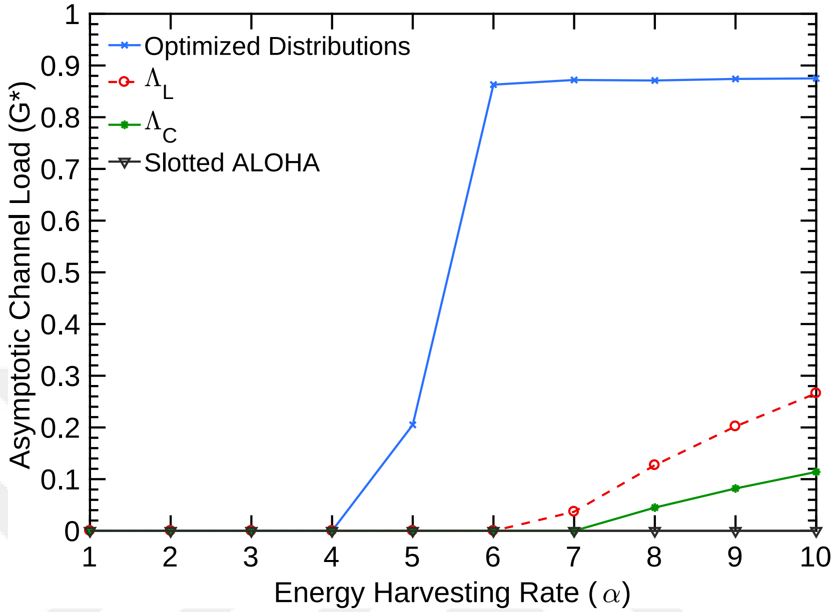

Figure 3.8: Comparison of the resulting maximum asymptotic channel loads of the target PLR=10^{-2} based optimized distributions for different EH rates with an activity probability of 1.

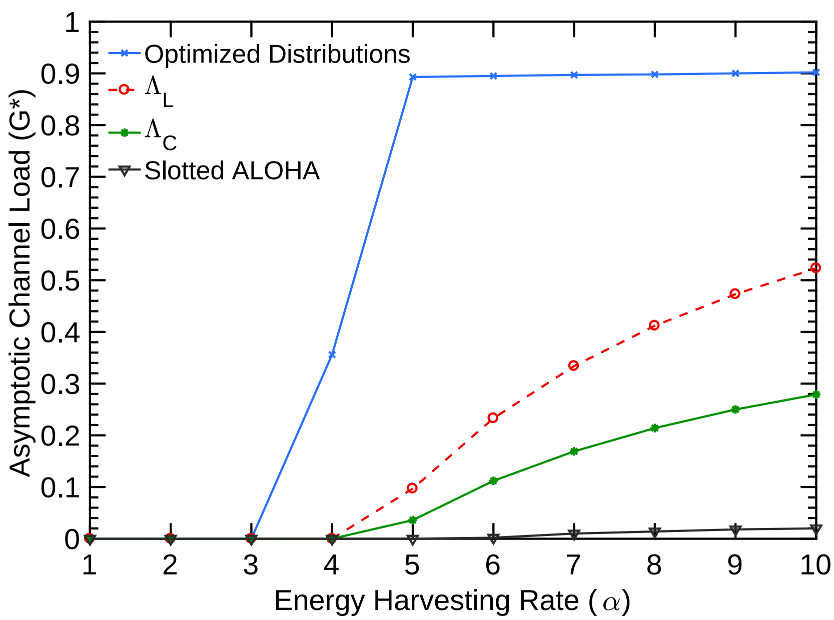

Figure 3.9: Comparison of the resulting maximum asymptotic channel loads of the target PLR=3.10^{-2} based optimized distributions for different EH rates with an activity probability of 1.

3.5 Chapter Summary

In this chapter, with the aim of extending the repetition based frame slotted ALOHA schemes on uncoordinated multiple access to EH devices, we have proposed a new scheme called EH-IRSA which is based on IRSA for a network of EH nodes. We analyzed the proposed scheme for the case in which each user has a unit-sized battery. The idea is similar to IRSA, with the difference that when battery of a user is depleted, the user skips the selected slot since it is not able to send the replica in this particular slot. For the analysis, the collision channel and binary EH model for which a unit of battery is recharged with a certain probability in each slot is considered. We first show that the effect of the approximation (that the transmitted packets are uniform across a frame) is valid and the asymptotic analysis results fit well with the finite frame length simulations. Moreover, by optimizing the RD we can obtain substantial throughput gains with respect to the optimized RD of IRSA without EH considerations.

Chapter 4

EH-IRSA with Finite Battery Capacity

In this chapter, we analyze the newly proposed EH-IRSA scheme for the case where the battery capacity B is greater than one unit. Although the model and our basic approach are similar, there are significant differences in the computation of the ERDs complicating the analysis. By emphasizing the differences, we propose an approach to obtain asymptotic performance of a given repetition distribution for a finite-sized battery. Then, we optimize the RDs using this new approach for the cases where complexity is reasonably low and utilizing Monte Carlo simulations for the more complicated scenarios. Finally, we compare the obtained asymptotic results with the finite frame length simulations.

The chapter is organized as follows. In Section 4.1, the differences of the system model with the one in Chapter 3 are given. The convergence analysis of the proposed EH-IRSA scheme for the finite-sized battery case is presented in 4.2. In Section 4.3, by using the proposed methodology and Monte Carlo simulations separately, several optimized RDs are obtained and their performances are compared with those of CRDSA and IRSA (optimized without the EH considerations), and throughput gain of the proposed solution within the EH framework is demonstrated. The summary of the chapter is provided in Section 4.4.

4.1 System Model

In the new system model, the only difference (with respect to the one in Chapter 3) is the battery capacity. Accordingly, we update the energy level change equations in each slot, and keep the definitions and channel model the same as those in Chapter 3.

The transmitting nodes with EH capability are equipped with a battery of capacity $B\delta$. Each transmission of a replica consumes δ energy. At any time slot an energy of δ units arrive with a probability p_c which is used to recharge the battery of each node (if it is not full) independently of the other time slots and users. We take $\delta = 1$ for the simplicity without any loss of generality.

Recall that E_s is the amount of energy at the battery at the start of the s^{th} slot. If there is no transmission at slot s, we have

$$E_{s+1} = \begin{cases} E_s + 1 & \text{with probability } p_c \text{ if } E_s < B, \\ E_s & \text{with probability } p_{nc}, \\ E_s & \text{if } E_s = B. \end{cases}$$

If there is a packet transmission at slot s, the amount of energy at the $(s+1)^{th}$ slot is given by

$$E_{s+1} = \begin{cases} E_s & \text{with probability } p_c \text{ if } E_s < B, \\ E_s - 1 & \text{with probability } p_c \text{ if } E_s = B, \\ E_s - 1 & \text{with probability } p_{nc}, \end{cases}$$

by noting the unit energy consumed in the transmission.

4.2 Convergence Analysis

The density evolution part of the convergence analysis is the same as the unit-sized battery case studied in Chapter 3. We again use the convergence analysis equations of IRSA with the assumption of that the received replicas at the receiver are uniformly distributed over the time slots. However, the previous ERD calculations are not valid in this case since the replica transmissions are not independent from the previous energy levels and transmissions as in the unit-sized battery case requiring a new development.

4.2.1 Effective Repetition Distribution

We adopt the same ERD calculation approach for a battery of higher capacity ($B > 1$). In the unit-sized case, the battery is recharged within i time slots with probability $1 - p_{nc}^{d_i}$, and does not get recharged with probability $p_{nc}^{d_i}$. These probabilities are also success and failure probabilities of the packets, i.e., $\Pr\{S_i = 1\}$ and $\Pr\{S_i = 0\}$, respectively. For the conversion of RD to ERD in the unit-sized battery case, we average the multiplication of l success and $k - l$ failure probabilities over the time slot separation (distance) selections to find the asymptotic average probabilities of l active packets over the k trials as done in (3.11).

In the multi-level battery scenario, however, the state of the battery also affects the number of active packets. We consider a probability tree to calculate the cases with specific energy arrivals, providing l active replicas over k replicas since it is clearly different than the multiplication of success and failure probabilities.

As an example, for a battery capacity of two ($B = 2$), we have 3 cases: no energy arrival, one energy arrival and more than one energy arrivals which have probabilities $p_{nc}^{d_i}$, $d_i p_c p_{nc}^{d_i - 1}$ and $1 - p_{nc}^{d_i} - d_i p_c p_{nc}^{d_i - 1}$ through d_i time slots, respectively. In the probability tree, we denote the current energy state by E, the current number of distances past by $K \in [0, k]$ and the current active packets by $L \in [0, K]$ as shown in Figure 4.1. The states are sampled just after trying to send a replica at the selected slot.

In the example given in Figure 4.1, $k = 2$, $B = 2$, and at the beginning of a frame there is no energy in the battery, i.e., $\Pr\{E_0 = 0\} = 1$. Note that the probability of being in the state $K = 1, L = 0, E = 1$ is 0. The probability of

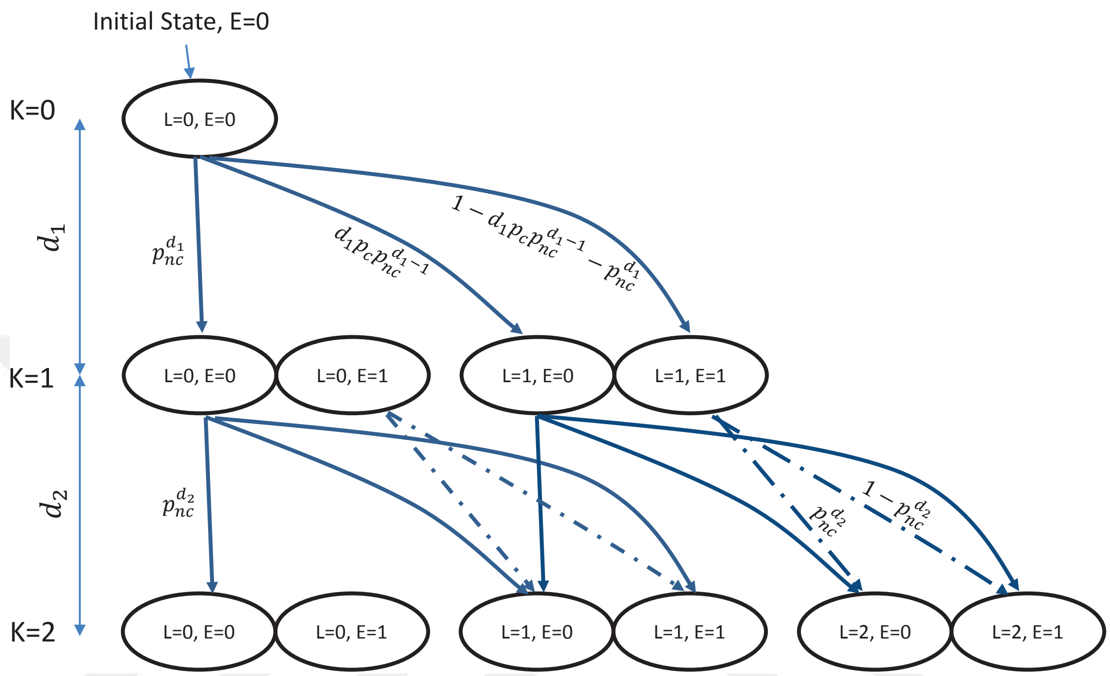

Figure 4.1: Probability tree diagram with 2 replicas, a battery size of 2 with an initial energy of 0 at the beginning of the frame.

sending no active packets after the first two distances is the multiplication of the probabilities of transitions between $L = 0, E = 0$ cases with increasing K values, which is $p_{nc}^{d_1+d_2}$. The probabilities are added at the nodes and multiplied through the arrows. The probability of sending one active replica over two selected slots is the sum of the cases with $L = 1$ at $K = 2$. From the tree, we can calculate that the probability of the state $K = 2, L = 1, E = 0$ as $p_{nc}^{d_1} . d_2 p_c p_{nc}^{d_2-1} + d_1 p_c p_{nc}^{d_1-1} . p_{nc}^{d_2}$. The probability of the state $K = 2, L = 1, E = 1$ is $p_{nc}^{d_1} . (1 - d_2 p_c p_{nc}^{d_2-1} - p_{nc}^{d_2})$.

Since the final state probabilities are calculated in terms of the distance vector $\boldsymbol{d}$, to obtain the final results in terms of α, they are averaged over all possible selections of distances, i.e., $\sum_{\boldsymbol{d}_1^k}(\cdot)$, and then, they are calculated asymptotically to find the probability (as a function of α) of having l active replicas over k total replicas, hence the ERD. For instance, we add the probabilities of states $K = 2, L = 1, E = 1$ and $K = 2, L = 1, E = 0$ to find the case $K = 2, L = 1$ and obtain $g(2, 2, 1) = d_1 p_c p_{nc}^{d_1-1} p_{nc}^{d_2} + p_{nc}^{d_1} - p_{nc}^{d_1+d_2}$ where $g(B, K, L)$ denotes the probability of L active replicas over K packets with $E = 0$ initially and battery capacity B. For the given case, we derive $\bar{\phi}_{l=1}^{k=2}$ using $g(2,2,1)$,

$$\begin{aligned}
\bar{\phi}_{l=1}^{k=2} &= \lim_{\substack{N\to\infty \\ p_c\to 0 \\ Np_c=\alpha}} \Pr\{\boldsymbol{d}\} \sum_{\boldsymbol{d}_1^2} g(2,2,1), \\
&= \lim_{\substack{N\to\infty \\ p_c\to 0 \\ Np_c=\alpha}} \Pr\{\boldsymbol{d}\} \sum_{\boldsymbol{d}_1^2} \left(p_{nc}^{d_1} - p_{nc}^{d_1+d_2} + p_c d_1 p_{nc}^{d_1+d_2-1}\right), \\
&= f(2,1) - f(2,2) - f^{(1)}(2,2)\frac{\alpha}{2},
\end{aligned} \tag{4.1}$$

where $f^{(i)}(k,r)$ is the ith derivative of $f(k,r)$ with respect to α. In (4.1), the conversion of the first two terms of $g(2,2,1)$ to f function is obvious. For the third term, we have

$$f(2,2) = \lim_{\substack{N\to\infty \\ p_c\to 0 \\ Np_c=\alpha}} \frac{1}{\binom{N}{k}} \sum_{\boldsymbol{d}_1^2} p_{nc}^{d_1+d_2} \tag{4.2}$$

and

$$\begin{aligned}
f^{(1)}(2,2) &= \lim_{\substack{N\to\infty \\ p_c\to 0 \\ Np_c=\alpha}} \frac{1}{\binom{N}{k}} \sum_{\boldsymbol{d}_1^2} -\frac{1}{N}(d_1+d_2) p_{nc}^{d_1+d_2-1} \\
&= \lim_{\substack{N\to\infty \\ p_c\to 0 \\ Np_c=\alpha}} \frac{1}{\binom{N}{k}} \sum_{\boldsymbol{d}_1^2} -\frac{1}{N} 2 d_1 p_{nc}^{d_1+d_2-1} \\
&= \lim_{\substack{N\to\infty \\ p_c\to 0 \\ Np_c=\alpha}} \frac{1}{\binom{N}{k}} \sum_{\boldsymbol{d}_1^2} -\frac{p_c}{\alpha} 2 d_1 p_{nc}^{d_1+d_2-1} \\
&= -\frac{2}{\alpha} \lim_{\substack{N\to\infty \\ p_c\to 0 \\ Np_c=\alpha}} \frac{1}{\binom{N}{k}} \sum_{\boldsymbol{d}_1^2} d_1 p_c p_{nc}^{d_1+d_2-1}
\end{aligned} \tag{4.3}$$

by the symmetry of the distances. In a similar way, all the terms are calculated in terms of $f(k,r)$ defined in (3.14) for any $\bar{\phi}_l^k$ for different battery capacities.

For the generalization of the method, we first define e_i^B that is the i unit recharging probability of a battery with capacity B in a distance d as

$$e_i^B = \begin{cases} \binom{d}{i} p_c^i p_{nc}^{d-i} & i \leq B, \\ 1 - \sum_{i=0}^{B} \binom{d}{i} p_c^i p_{nc}^{d-i} & i = B \\ 0 & \text{otherwise.} \end{cases}$$

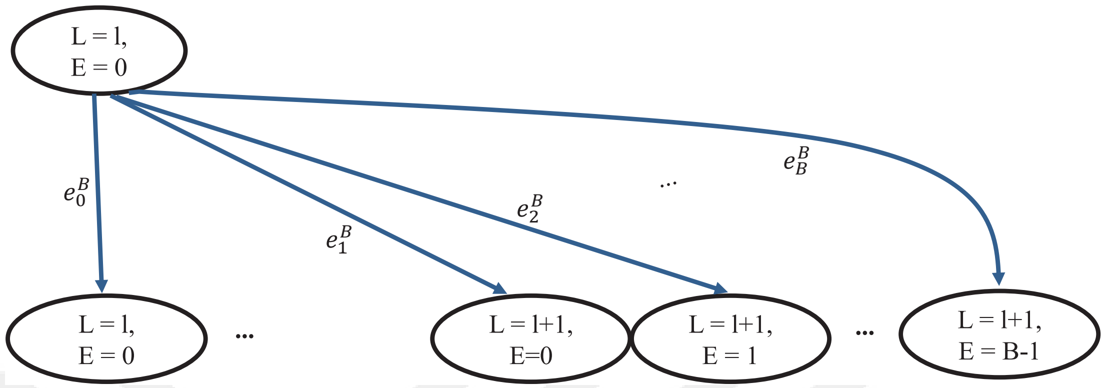

Figure 4.2: Generic probability tree diagram transitions for a zero energy state.

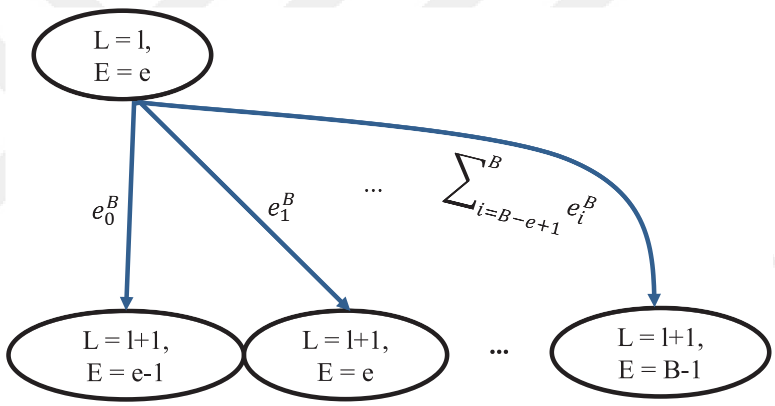

Figure 4.3: Generic probability tree diagram transitions for an energy state greater than zero.

Next, we need to find the behavior of the state transitions. The transitions have two different behaviors for the states with $E = 0$ and $E \geq 0$, independent of K and L as it is observed Figure 4.1. For the states with $E = 0$ and $E > 0$, the state transitions are shown in Figure 4.2 and Figure 4.3, respectively. The main difference is that if a user has no energy at a state, it may not be able to send a replica, and stays at l active packets. If it has energy, it definitely increases the number of active replicas by 1 at this step. We can write a distance probability transition matrix to find the final state probabilities in a compact form. For instance, we define the probabilities of the states as $s_{K,L,E}$ for $K \in [0, k]$, $L \in [0, k]$ and $E \in [0, B]$, noting that there are a total of $(k+1)(k+1)(B+1)$ many states. Then, we can write the state transition probabilities from a state with $K = j$, $L = l$, $E = 0$ (no energy) and by multiplying a state with the vector of transition probabilities, we can obtain the probabilities of all the resulting states after a transition, i.e.,

$$
\begin{aligned}
&s_{j,l,0}.[e_0^B \quad 0 \quad \dots \quad 0 \quad e_1^B \quad e_2^B \quad \dots \quad e_B^B] = \\
&\qquad [s_{j+1,l,0} \quad s_{j+1,l,1} \quad \dots \quad s_{j+1,l,B} \quad s_{j+1,l,0} \quad s_{j+1,l+1,0} \quad \dots \quad s_{j+1,l+1,B}]. \qquad (4.4)
\end{aligned}
$$

where a set of states with $K = j$ and $E = 0$ are multiplied with a transformation vector and the probabilities of the new states at $K = j + 1$ are obtained.

In a similar way, to obtain the state transition matrix, we first write the initial state probabilities ($K = 0$) without an energy limitation (instead of the example above, we consider all the states at $K = 0$) in a vector form, including the zero probability hidden states that are not connected to the next level of states ($K = 1$), i.e., the states with $L = 1, \dots, k$ and $K = 0$, we can write

$$
\begin{aligned}
\boldsymbol{P} &= [s_{0,0,0} \quad s_{0,0,1} \quad \dots \quad s_{0,0,B} \quad 0 \quad \dots \quad 0]_{1\times(B+1)(k+1)} \qquad (4.5)\\
&= [\Pr\{E_0 = 0\} \quad \Pr\{E_0 = 1\} \quad \dots \quad \Pr\{E_0 = B\} \quad 0 \quad \dots \quad 0]. \qquad (4.6)
\end{aligned}
$$

The distance transition matrix that transforms the state probabilities from K to $K + 1$ can be written as

$$
\mathbf{T}(d) = \begin{bmatrix}
T_{s_1} & T_{s_2} & \mathbf{0} & \dots & \mathbf{0} & \mathbf{0} & \mathbf{0} \\
\mathbf{0} & T_{s_1} & T_{s_2} & \dots & \mathbf{0} & \mathbf{0} & \mathbf{0} \\
 & \vdots & & \ddots & & \vdots & \\
\mathbf{0} & \mathbf{0} & \mathbf{0} & \dots & T_{s_1} & T_{s_2} & \mathbf{0} \\
\mathbf{0} & \mathbf{0} & \mathbf{0} & \dots & \mathbf{0} & T_{s_1} & T_{s_2} \\
\mathbf{0} & \mathbf{0} & \mathbf{0} & \dots & \mathbf{0} & \mathbf{0} & \mathbf{0}
\end{bmatrix}_{(k+1)(B+1)\times(k+1)(B+1)}
$$

where

$$
T_{s_1} = \begin{bmatrix}
e_0^B & 0 & \dots & 0 & 0 \\
0 & 0 & \dots & 0 & 0 \\
\vdots & \vdots & \ddots & \vdots & \vdots \\
0 & 0 & \dots & 0 & 0
\end{bmatrix}_{(B+1)\times(B+1)}
$$

and

$$T_{s_2} = \begin{bmatrix} e_1^B & e_2^B & \dots & e_{B-1}^B & e_B^B & 0 \\ e_0^B & e_1^B & \dots & e_{B-2}^B & e_{B-1}^B + e_B^B & 0 \\ 0 & e_0^B & \dots & e_{B-3}^B & e_{B-2}^B + e_{B-1}^B + e_B^B & 0 \\ \vdots & \vdots & \ddots & \vdots & \vdots & \vdots \\ 0 & 0 & \dots & e_0^B & \sum_{i=1}^B e_i^B & 0 \\ 0 & 0 & \dots & 0 & 1 & 0 \end{bmatrix}_{(B+1)\times(B+1)}.$$

where T_{s_1} and T_{s_2} are also functions of d. Each of the final state ($K = k$) probabilities $\boldsymbol{W}$ can then be calculated by using $\boldsymbol{W} = \boldsymbol{P}\prod_{i=1}^k \boldsymbol{T}(d_i)$ which we simply denote as $\boldsymbol{W} = \boldsymbol{PT}^k$. For the explained example of $B = 2$, $k = 2$ and initial energy $E = 0$, we calculate the end probabilities with this approach as $\boldsymbol{PT}^2$, where $\boldsymbol{P} = [1\ 0\ \dots\ 0]$ and distance transition matrix

$$T_s = \begin{bmatrix} e_0^2 & 0 & 0 & e_1^2 & e_2^2 & 0 \\ 0 & 0 & 0 & e_0^2 & e_1^2 + e_2^2 & 0 \\ 0 & 0 & 0 & 0 & 1 & 0 \end{bmatrix}.$$

After finding the final probabilities in terms of the distances, we average the probabilities over the distances asymptotically through $\lim_{\substack{N\to\infty \\ p_c\to 0 \\ Np_c=\alpha}} \Pr\{\boldsymbol{d}\}\sum_{\boldsymbol{d}_1^2}\boldsymbol{W}$ and find the ERDs of the multiple battery systems with the help of symbolic computation tools.

Although it is possible to obtain the corresponding ERD of a given RD and average initial energy probabilities (of each frame) with symbolic computation tools, a further simplification in terms of conversion to f function can be interesting for future work. We note that the initial probability matrix I which depends on the RD and α is also required for the exact analysis of the system.

In the numerical examples section, we verify the validity of the approach for the adopted approximation by comparing the analytical results with those of Monte Carlo simulations and provide the throughputs that can be achieved using the developed methodology.

4.3 Numerical Examples

In this chapter, we have provided an asymptotic analysis methodology for EH-IRSA with a finite-sized battery. In Table 4.1, for $B = 2$, $k = 4$ and $E_0 = 0$, we present an example of the result and validate it by comparing the results for fixed $\alpha = 5$ using Monte Carlo simulations for the same scenario.

Above comparisons indicate that the analysis technique conforms with the simulations. However, noting that for larger battery capacities, the analysis requires a very high level of computations, hence we resort to Monte Carlo based techniques to generate the ERDs from the given RDs, and use these ERDs to optimize the system throughput via the density evolution. We simulate these optimized distributions for finite frame length scenarios. In the optimizations, we choose the α values above the threshold that we have observed in the unit-sized battery case so that the maximum throughput is sufficiently high and the optimized distribution is not simply $\Lambda_{max} = x^8$ (assuming a maximum repetition degree of 8). Therefore, the optimization algorithm is run to obtain the maximum G^* providing the PLR that is not above the target PLR.

For fixed initial energies at the beginning of each frame, the probability of l active packets over k packets up to a maximum repetition order 8 is generated, and their linear combinations are used to calculate the corresponding ERDs from

Table 4.1: $\bar{\phi}_l^k$ values for $E_0 = 0$, $k = 4$ and $B = 2$, simulation results are averages of 10^6 repetitions with a finite frame length of $N = 1000$.

l	Symbolic Solution	$\alpha = 5$	Simulation
0	$\frac{24}{\alpha^4} - \mathrm{e}^{-\alpha}\left(\frac{4}{\alpha} + \frac{12}{\alpha^2} + \frac{24}{\alpha^3} + \frac{24}{\alpha^4}\right)$	0.0282	0.0273
1	$\frac{24}{\alpha^3} - \frac{24}{\alpha^4} - \mathrm{e}^{-\alpha}\left(\frac{8}{\alpha} + \frac{12}{\alpha^2} - \frac{24}{\alpha^4} + 3\right)$	0.1196	0.1172
2	$\frac{12}{\alpha^2} + \frac{24}{\alpha^3} - \frac{288}{\alpha^4} + \mathrm{e}^{-\alpha}\left(\frac{24}{\alpha} - \frac{3\,\alpha}{5} + \frac{108}{\alpha^2} + \frac{264}{\alpha^3} + \frac{288}{\alpha^4} + 2\right)$	0.2832	0.2812
3	$\frac{4}{\alpha} + \frac{12}{\alpha^2} - \frac{240}{\alpha^3} + \frac{624}{\alpha^4} - \mathrm{e}^{-\alpha}\left(\frac{84}{\alpha^2} - \frac{4\,\alpha}{5} + \frac{\alpha^2}{30} + \frac{384}{\alpha^3} + \frac{624}{\alpha^4} - 4\right)$	0.3566	0.3583
4	$\frac{192}{\alpha^3} - \frac{24}{\alpha^2} - \frac{4}{\alpha} - \frac{336}{\alpha^4} - \mathrm{e}^{-\alpha}\left(\frac{\alpha}{5} + \frac{12}{\alpha} - \frac{\alpha^2}{30} - \frac{144}{\alpha^3} - \frac{336}{\alpha^4} + 3\right) + 1$	0.2123	0.2160

the RDs as in the unit-battery case. In the example, the battery capacity is two units ($B = 2$), all the users are active ($\pi = 1$), and the EH rate is two ($\alpha = 2$). The initial energy is also fixed at $E = 2$, i.e., the battery is full at the start of each frame which can be justified assuming a sparse activity. For a target PLR=10^{-2}, we obtain the optimized distribution $\Lambda_4(x) = 0.01x^1 + 0.26x^2 + 0.05x^6 + 0.20x^7 + 0.48x^8$ with the corresponding ERD $\widetilde{\Lambda}_4(x) = 0.01x^1 + 0.42x^2 + 0.26x^3 + 0.19x^4 + 0.09x^5 + 0.03x^6$. In Figure 4.4, $\Lambda_4(x)$ is compared with the Λ_L and Λ_C and it is observed that the optimization provides some gain with respect to Λ_L while the finite frame length simulations fit reasonably well with the asymptotic results.

We next consider the case where there is no energy at the beginning of each frame ($E = 0$) for an EH rate $\alpha = 6$ with the same battery capacity $B = 2$. The optimization algorithm is run for a target PLR=10^{-2} which results in the distribution $\Lambda_5(x) = 0.12x^4 + 0.08x^5 + 0.15x^6 + 0.14x^7 + 0.51x^8$ with the corresponding ERD $\widehat{\Lambda}_5(x) = 0.04x^1 + 0.13x^2 + 0.23x^3 + 0.27x^4 + 0.19x^5 + 0.10x^6 + 0.03x^7 + 0.01x^8$. In Figure 4.5, the asymptotic and finite frame length performances are shown. It is observed that Λ_5 provides more gain than the previous case in the finite size simulations with respect to $\Lambda_L(x)$. We attribute the addition of improvement to the following: The low initial energies result in more difference between the ERD and RD while the difference was smaller in the previous example, hence Λ_L performed well. We also observe that, for low initial energies, the asymptotic performances do not comply well with the finite size simulations which is caused from the uniformity assumption of ERDs we make for the density evolution analysis. With an initial energy of 0 at the beginning of each frame, the distribution of ERDs deviate more with respect to the uniform distribution, hence the users cannot send replicas in the first part of the frame equally well with the rest of the frame. This results in the higher number of packets for the rest of the frame with respect to the uniform distribution and lower number of packets for the first part of the frame. However, the optimization still works reasonably well.

We perform a Monte Carlo based optimization in which the initial energy is averaged over all possible initial energies and each RD is converted to an ERD via simulations. For a setup with $\pi = 1$, $\alpha = 4$, $B = 3$, we optimize the RD for a target $PLR = 3.10^{-2}$ and obtain the distribution

$\Lambda_6(x) = 0.14x^2 + 0.40x^3 + 0.01x^4 + 0.31x^6 + 0.14x^8$ with the corresponding ERD $\widetilde{\Lambda}_6(x) = 0.02x^0 + 0.07x^1 + 0.24x^2 + 0.37x^3 + 0.11x^4 + 0.10x^5 + 0.08x^6 + 0.01x^7$. We illustrate the asymptotic and finite frame length simulation results of $\Lambda_6(x)$ with $\Lambda_L(x)$ and $\Lambda_C(x)$ for the given case in Figure 4.6. We observe that $\Lambda_6(x)$ provides a maximum offered load $G^* = 0.907$ with a target $PLR = 3.10^{-2}$. From these Monte Carlo based results, we conclude that the optimization approach we adopt is valid and further simplification and complexity reduction in the proposed analytical process promise substantial gains with respect to the existing solutions.

Lastly, we investigate the effect of the battery size for the proposed optimization. To do this, we also use the Monte Carlo based optimization methodology without a certain initial energy at the beginning of a frame. For a target PLR of 3.10^{-2}, we optimize distributions for each of the cases with a different battery capacity while α is fixed at 5. In Figure 4.7, the relation between battery size and maximum asymptotic channel load is shown. Note that the optimized distributions are not the trivial solution Λ_{max}. It can be seen that, for increasing size of the battery, the performance that can be gained via the proposed optimization decreases and the IRSA optimization without EH (Λ_L) becomes valid. Therefore, with a high battery capacity, the EH consideration in the convergence analysis becomes less significant and the original IRSA based solution performs well as expected.

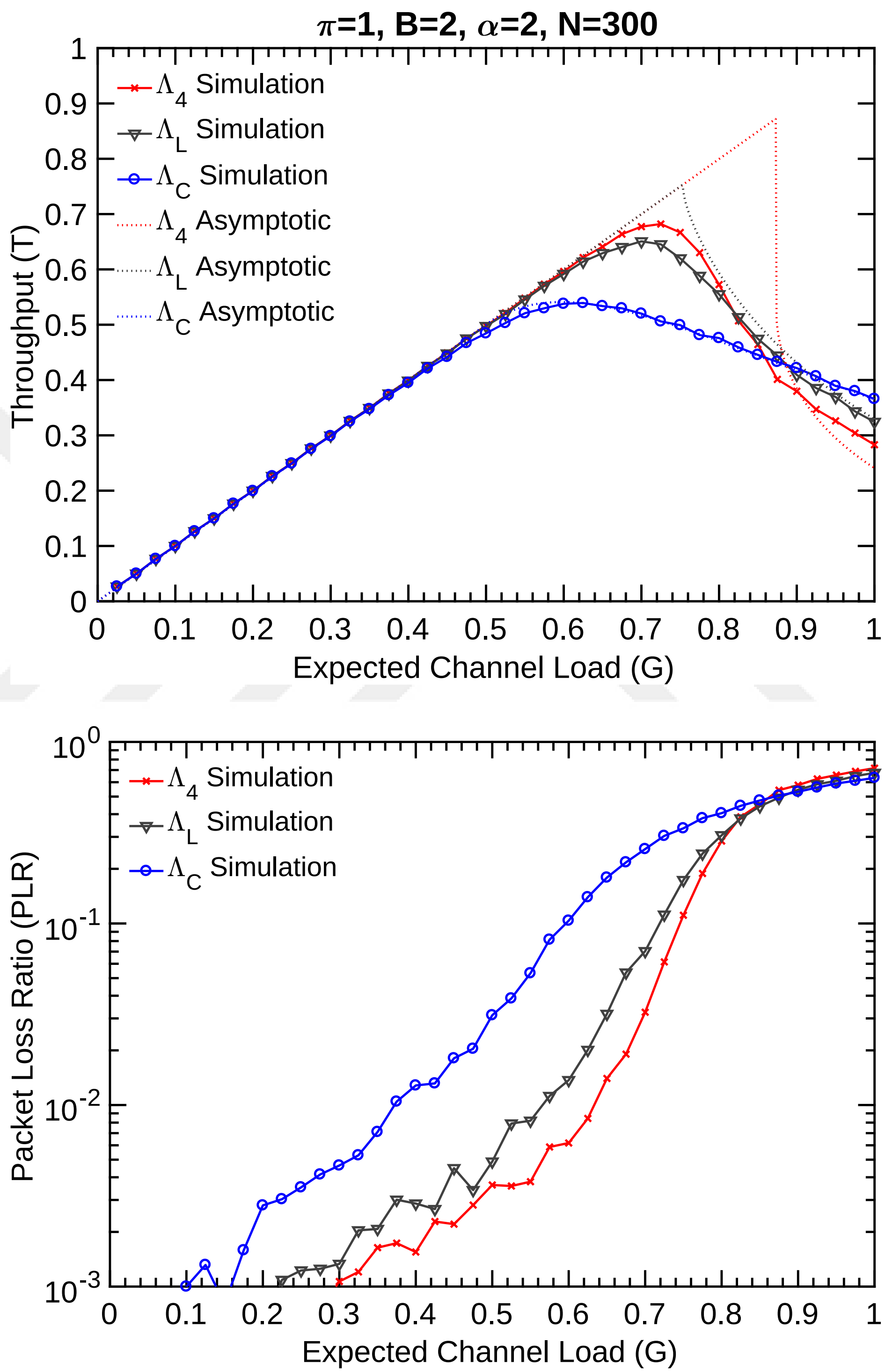

Figure 4.4: Comparison of the resulting throughput of the distributions for an EH rate of 2, an activity probability of 1, a battery capacity of 2, and an initial energy of 2 at each frame.

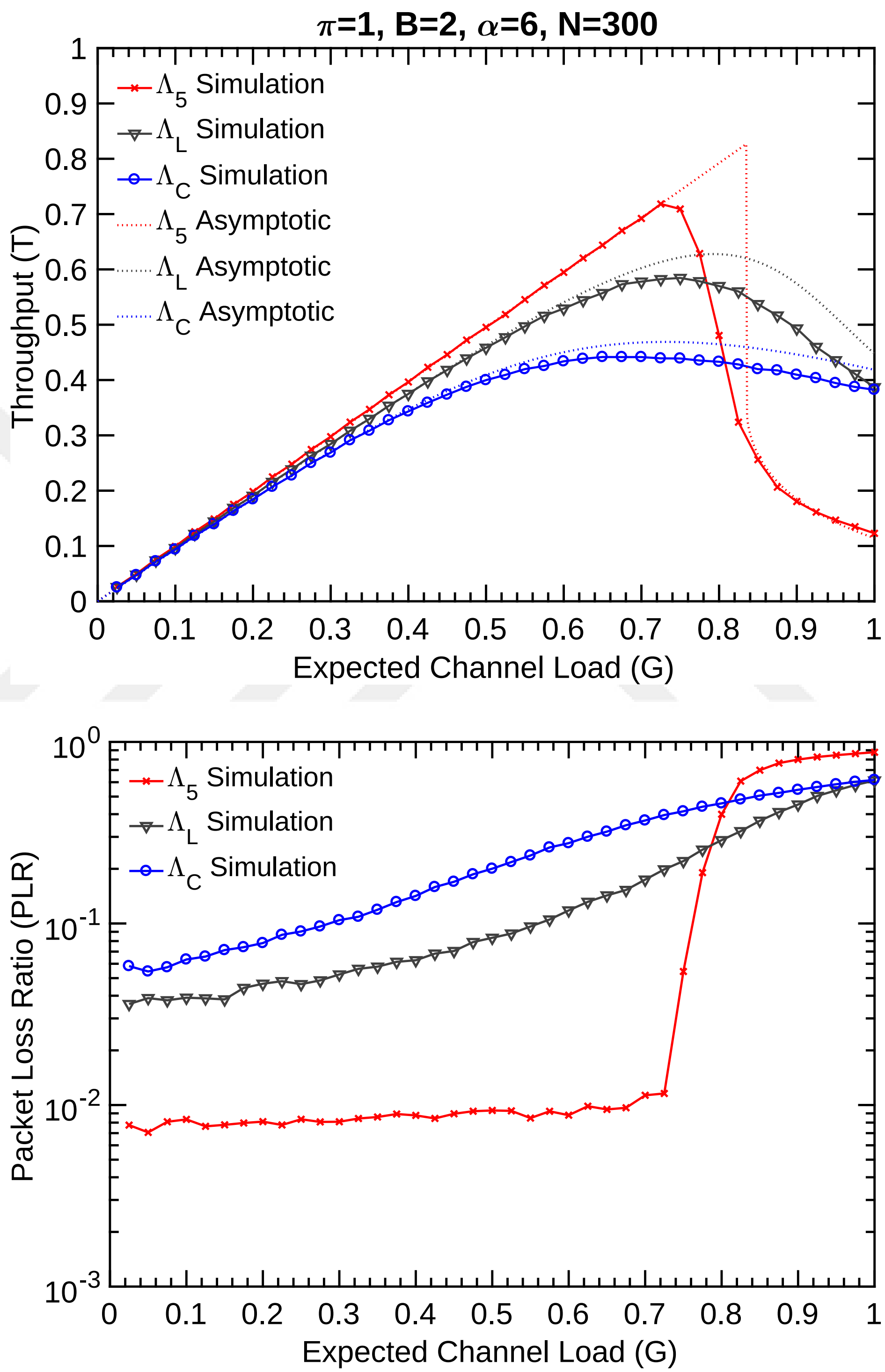

Figure 4.5: Comparison of the resulting throughput of the distributions for an EH rate of 2, an activity probability of 1, a battery capacity of 2, and an initial energy of 0 at each frame.

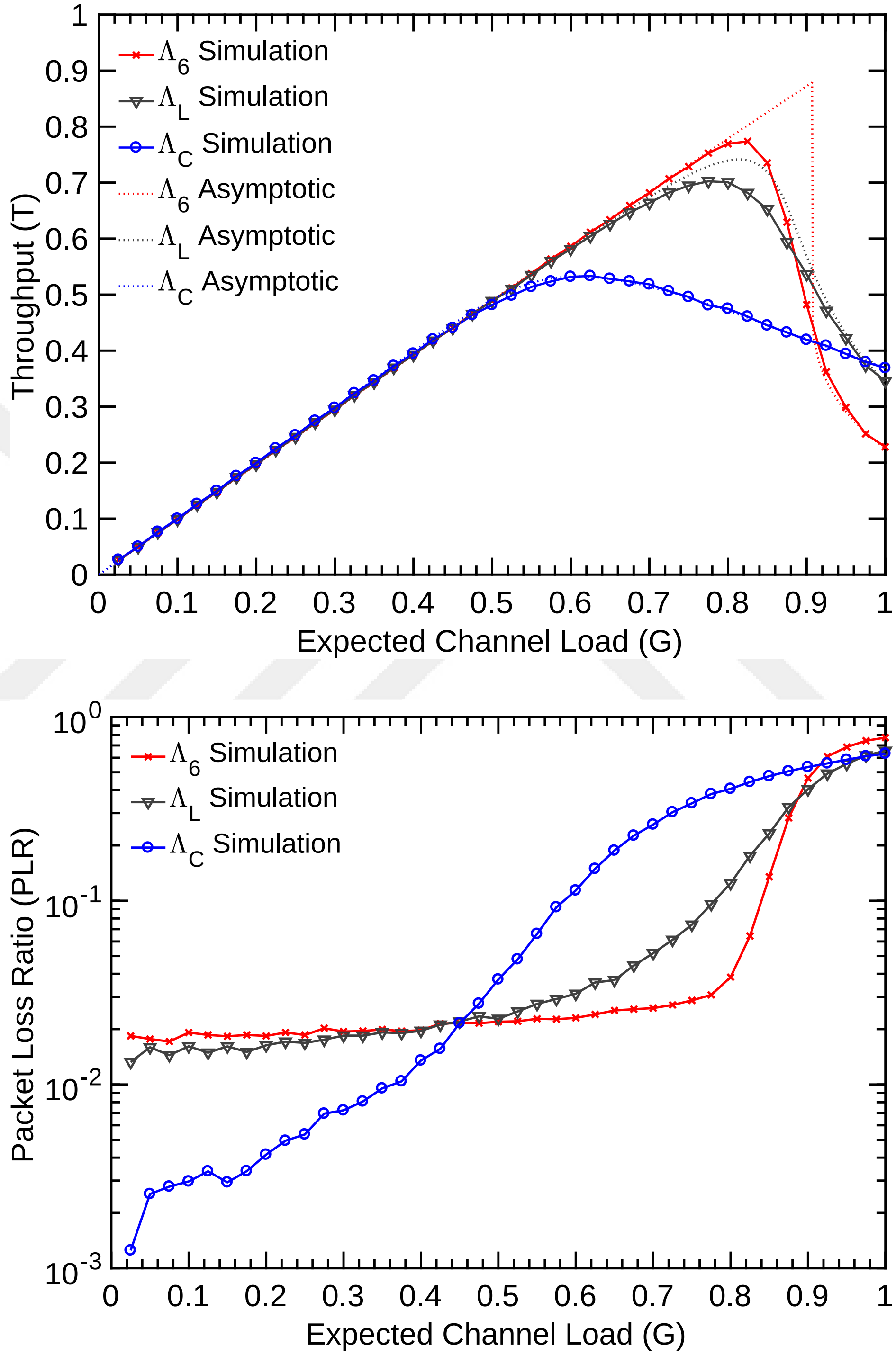

Figure 4.6: Comparison of the resulting throughput of the distributions for an EH rate of 4, an activity probability of 1, a battery capacity of 3 averaged over all possible initial energy states.

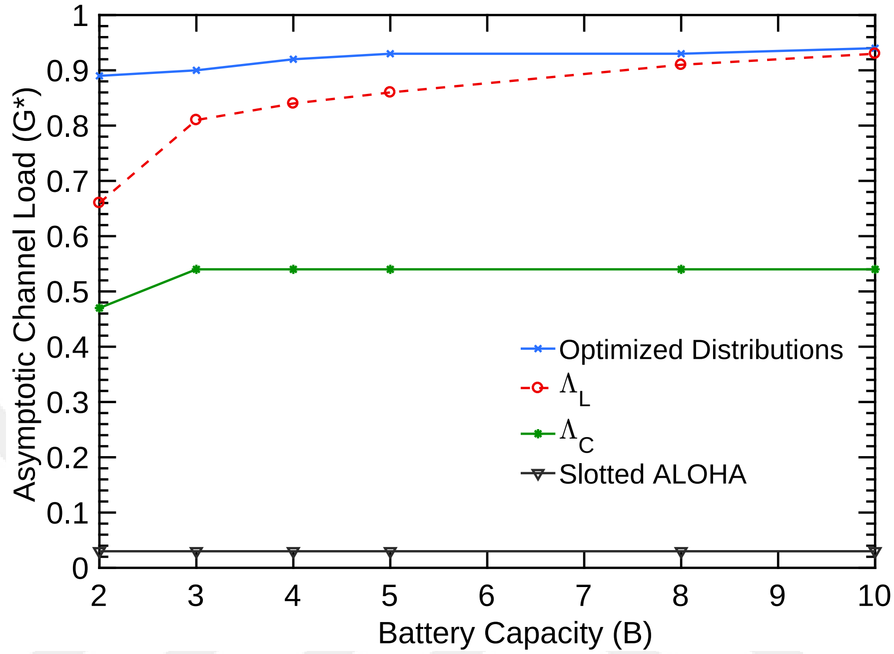

Figure 4.7: Comparison of the resulting maximum asymptotic channel loads for the target PLR=3.10^{-2} based optimized distributions for different battery capacities ($\alpha = 5$).

4.4 Chapter Summary

In this chapter, we have analyzed the EH-IRSA for the case in which each user has a battery with capacity B. To do this, we update the energy model and convergence analysis techniques used in Chapter 3. We illustrate the probability calculations required in the RD to ERD conversion on a probabilistic graphical model, and propose a matrix multiplication for the calculation. Obtaining the proposed analysis based and Monte Carlo based optimization results, we compare the asymptotic performance with those of the finite frame length simulations, and show that for the multiple battery capacity case too, the EH-IRSA provides considerable throughput gains with respect to the existing solutions.

Chapter 5

Conclusions and Future Research Directions

Modern random access schemes, specifically Coded Slotted ALOHA and similar schemes adopting SIC among different time slots show promising performance in terms of throughput without a coordination among the users. With the aim of achieving high throughput performances of these schemes in an EH setting, in this thesis, we propose an IRSA based scheme accommodating EH nodes in the random access system.

The proposed EH-IRSA scheme is a frame based ALOHA scheme in which the users send multiple copies of their packets for the corresponding frames. The collisions are resolved using SIC across frames with the use of the copies. Considering the EH system, the users have limited battery capacities and a unit of the battery is recharged with a certain probability in each slot. The nodes use a realization of a random variable to determine the number of replicas to be sent in each frame. The number of actually transmitted replicas are different than the number of the intended ones due to the energy constraints. Therefore, we derive the distribution of the number of replicas that are actually transmitted as a function of the distribution of the number of replicas that the users try to send as a function of the EH rate. Using the new distribution of the transmitted packets along with the asymptotic density evolution analysis developed for IRSA, we evaluate the performance of the proposed scheme and optimize the distributions of the repetitions. We demonstrate via examples that these optimized distributions provide high throughput values without a coordination and offer gains with respect to the existing schemes which do not consider EH.

There are a number of possible research directions. For instance, the accuracy of the analysis may be improved by getting rid of the approximation that the received packets are uniform. To do this, it may be possible to provide a different way of slot selection which provides an exact uniform distribution at the receiver. Moreover, the complexity of the proposed analysis for the finite battery case is still high. It may be feasible to extend the properties of the f function and obtain a faster analysis method as considered in the unit-sized battery scenario. The initial energy state probabilities of each frame are also needed to be derived for a continuously working scheme. Furthermore, the other RA based EH schemes may be used with the same battery and EH model and the resulting schemes can be compared to show the advantages and disadvantages of EH-IRSA.

While our approach and results provide a basis for different EH models, for further research, more generic and realistic EH models with memory and correlation among the users in the energy arrivals may also be considered. Another research direction may be the following: the single EH rate selected for all the users can be varied among users resulting in new optimization methodologies. Moreover, the EH-IRSA scheme may also be optimized for the different and more complicated channel models with physical layer concerns instead of using the simple collision channel. For instance, a Rayleigh fading channel model with a receiver having the capability of benefiting from the capture effect may be considered. Such a physical layer optimization may provide higher throughputs and less number of replicas per user improving the system efficiency.

We also note that, in the present work, we do not take energy efficiency into consideration. Thus, number of replicas transmitted may be limited for the EH-IRSA scheme. Another research direction can be to propose a CSA-like EH scheme by limiting the total energy that may be spent to send a packet and find the maximum rates allowing highly efficient communications. Such more efficient communication schemes may get rid of the requirement for the slot synchronization. Finally, noting that an unslotted RA scheme benefiting from the SIC process is proposed in [39], the EH counterparts of this scheme may also be considered with specific solutions considering EH.

Bibliography

[1] N. Abramson, "The ALOHA system," in *AFIPS '70 Fall Jt. Comput. Conf.*, vol. 37, Houston, Texas, USA, Nov. 1970, p. 281.

[2] L. Roberts, "ALOHA packet system with and without slots and capture," *ACM SIGCOMM Comput. Commun. Rev.*, vol. 5, no. 2, pp. 28–42, Apr. 1975.

[3] S. Li, L. D. Xu, and S. Zhao, "The internet of things: a survey," *Inf. Syst. Front.*, vol. 17, no. 2, pp. 243–259, Oct. 2015.

[4] NGMN Alliance, "5G White Paper," *Next Gener. Mob. Networks, White Pap.*, pp. 1–125, 2015.

[5] E. Paolini, G. Liva, and M. Chiani, "Coded slotted ALOHA: A graph-based method for uncoordinated multiple access," *IEEE Trans. Inf. Theory*, vol. 61, no. 12, pp. 6815–6832, Dec. 2015.

[6] G. L. Choudhury and S. S. Rappaport, "Diversity ALOHA – random access scheme for satellite communications," *IEEE Trans. Commun.*, vol. 31, no. 3, pp. 450–457, Mar. 1983.

[7] E. Casini, R. De Gaudenzi, and O. Del Rio Herrero, "Contention resolution diversity slotted ALOHA (CRDSA): An enhanced random access scheme for satellite access packet networks," *IEEE Trans. Wirel. Commun.*, vol. 6, no. 4, pp. 1408–1419, Apr. 2007.

[8] G. Liva, "Graph-based analysis and optimization of contention resolution diversity slotted ALOHA," *IEEE Trans. Commun.*, vol. 59, no. 2, pp. 477–487, Feb. 2011.

[9] R. Storn and K. Price, "Differential evolution - a simple and efficient heuristic for global optimization over continuous spaces," *J. Glob. Optim.*, vol. 11, no. 4, pp. 341–359, Dec. 1997.

[10] E. Paolini, G. Liva, and M. Chiani, "Graph-based random access for the collision channel without feedback: Capacity bound," in *IEEE Glob. Telecommun. Conf. (GLOBECOM)*, Houston, Texas, USA, Dec. 2011, pp. 1–5.

[11] M. Ivanov, F. Brannstrom, A. Graell I Amat, and P. Popovski, "Error floor analysis of coded slotted ALOHA over packet erasure channels," *IEEE Commun. Lett.*, vol. 19, no. 3, pp. 419–422, Mar. 2015.

[12] Z. Sun, Y. Xie, J. Yuan, and T. Yang, "Coded slotted ALOHA schemes for erasure channels," in *IEEE Int. Conf. Commun. (ICC)*, Kuala Lumpur, Malaysia, May 2016, pp. 1–6.

[13] H. C. Bui, J. Lacan, and M.-L. Boucheret, "Multi-slot coded ALOHA with irregular degree distribution," in *IEEE First AESS Eur. Conf. Satell. Telecommun. (ESTEL)*, Rome, Italy, Oct. 2012, pp. 1–6.

[14] H. C. Bui, J. Lacan, and M. L. Boucheret, "An enhanced multiple random access scheme for satellite communications," in *Wirel. Telecommun. Symp. (WTS*, vol. 2, London, UK, Apr. 2012, pp. 1–6.

[15] M. Ghanbarinejad and C. Schlegel, "Irregular repetition slotted ALOHA with multiuser detection," in *10th Annu. Conf. Wirel. On-Demand Netw. Syst. Serv. (WONS)*, Banff, Alberta, Canada, Mar. 2013, pp. 201–205.

[16] F. Clazzer, E. Paolini, I. Mambelli, and C. Stefanovic, "Irregular repetition slotted ALOHA over the Rayleigh block fading channel with capture," in *IEEE Int. Conf. Commun. (ICC)*, Paris, France, May 2017.

[17] R. De Gaudenzi, A. Mengali, and P.-D. Arapoglou, "Enhancing the physical layer of contention resolution diversity slotted ALOHA," *IEEE Trans. Commun.*, vol. PP, no. 99, pp. 1–1, 2017.

[18] S. Pfletschinger, M. Navarro, and G. Cocco, "Interference cancellation and joint decoding for collision resolution in slotted ALOHA," in *Int. Symp. Netw. Coding (NetCod)*, Aalborg Oest, Denmark, Jun. 2014, pp. 1–6.

[19] G. Interdonato, S. Pfletschinger, F. Vazquez-Gallego, J. Alonso-Zarate, and G. Araniti, "Intra-slot interference cancellation for collision resolution in irregular repetition slotted ALOHA," in *IEEE Int. Conf. Commun. (ICC)*, no. 978, London, UK, Jun. 2015, pp. 2069–2074.

[20] D. Jia, Z. Fei, H. Lin, J. Yuan, and J. Kuang, "Distributed decoding for coded slotted ALOHA," *IEEE Commun. Lett.*, vol. PP, no. 99, pp. 1–1, 2017.

[21] S. Ulukus, A. Yener, E. Erkip, O. Simeone, M. Zorzi, P. Grover, and K. Huang, "Energy harvesting wireless communications: A review of recent advances," *IEEE J. Sel. Areas Commun.*, vol. 33, no. 3, pp. 360–381, Mar. 2015.

[22] J. Jeon and A. Ephremides, "The stability region of random multiple access under stochastic energy harvesting," in *Proc. IEEE Int. Symp. Inf. Theory (ISIT)*, Saint-Petersburg, Russia, Jul. 2011, pp. 1796–1800.

[23] ——, "On the stability of random multiple access with stochastic energy harvesting," *IEEE J. Sel. Areas Commun.*, vol. 33, no. 3, pp. 571–584, Mar. 2015.

[24] A. M. Ibrahim, O. Ercetin, and T. Elbatt, "Stability analysis of slotted ALOHA with opportunistic RF energy harvesting," *IEEE J. Sel. Areas Commun.*, vol. 34, no. 5, pp. 1477–1490, May 2016.

[25] M. Moradian and F. Ashtiani, "Throughput analysis of a slotted ALOHA-based network with energy harvesting nodes," in *IEEE 23rd Int. Symp. Pers. Indoor Mob. Radio Commun. (PIMRC)*, Sydney, Australia, Sep. 2012, pp. 351–356.

[26] ——, “Sum throughput maximization in a slotted ALOHA network with energy harvesting nodes,” in *IEEE Wirel. Commun. Netw. Conf. (WCNC)*, Istanbul, Turkey, Apr. 2014, pp. 1585–1590.

[27] N. Michelusi and M. Zorzi, “Optimal adaptive random multiaccess in energy harvesting wireless sensor networks,” in *IEEE Trans. Commun.*, vol. 63, no. 4, Jun. 2015, pp. 1355–1372.

[28] F. Iannello, O. Simeone, and U. Spagnolini, “Dynamic framed-ALOHA for energy-constrained wireless sensor networks with energy harvesting,” in *IEEE Glob. Telecommun. Conf. (GLOBECOM)*, Miami, Florida, USA, Dec. 2010, pp. 1–6.

[29] F. C. Schoute, “Dynamic frame length ALOHA,” *IEEE Trans. Commun.*, vol. 31, no. 4, pp. 565–568, Apr. 1983.

[30] F. Iannello, O. Simeone, and U. Spagnolini, “Medium access control protocols for wireless sensor networks with energy harvesting,” *IEEE Trans. Commun.*, vol. 60, no. 5, pp. 1381–1389, May 2012.

[31] F. Iannello, O. Simeone, P. Popovski, and U. Spagnolini, “Energy group-based dynamic framed ALOHA for wireless networks with energy harvesting,” in *46th Annu. Conf. Inf. Sci. Syst. (CISS)*, Princeton, NJ, USA, Mar. 2012, pp. 1–6.

[32] S. Wu, Y. Chen, K. K. Chai, F. Vazquez-Gallego, and J. Alonso-Zarate, “Analysis and performance evaluation of dynamic frame slotted-ALOHA in wireless machine-to-machine networks with energy harvesting,” in *IEEE Glob. Telecommun. Conf. (GLOBECOM)*, Austin, Texas, USA, Dec. 2014, pp. 1081–1086.

[33] F. Vazquez-Gallego, J. Alonso-Zarate, and L. Alonso, “Reservation dynamic frame slotted-ALOHA for wireless M2M networks with energy harvesting,” *IEEE Int. Conf. Commun. (ICC)*, pp. 5985–5991, Sep. 2015.

[34] F. Vazquez-Gallego, J. Alonso-Zarate, A. M. Mandalari, O. Briante, A. Molinaro, and G. Ruggeri, "Performance evaluation of reservation frame slotted-ALOHA for data collection M2M networks," *20th Eur. Wirel. Conf. (EW)*, pp. 1–6, May 2014.

[35] K. Tutuncuoglu, O. Ozel, A. Yener, and S. Ulukus, "Binary energy harvesting channel with finite energy storage," in *Proc. IEEE Int. Symp. Inf. Theory (ISIT)*, Jul. 2013, pp. 1591–1595.

[36] ——, "The binary energy harvesting channel with a unit-sized battery," *IEEE Trans. Inf. Theory*, vol. 63, no. July 2013, pp. 1–31, Jul. 2017.

[37] D. Shaviv and A. Ozgur, "Capacity of the AWGN channel with random battery recharges," in *Proc. IEEE Int. Symp. Inf. Theory (ISIT)*, Hong Kong, Jun. 2015, pp. 136–140.

[38] D. Shaviv, P. M. Nguyen, and A. Ozgur, "Capacity of the energy-harvesting channel with a finite battery," *IEEE Trans. Inf. Theory*, vol. 62, no. 11, pp. 6436–6458, Nov. 2016.

[39] F. Clazzer and C. Kissling, "Enhanced contention resolution ALOHA - ECRA," *Proc. 9th Int. ITG Conf. Syst. Commun. Coding*, vol. 9, pp. 1–6, Nov. 2012.